

Analysis of Fundus Images to Detect Different Abnormalities Related to Hypertensive Retinopathy



Author

MUHAMMAD AHMAD

NUST201362749MSEEC61313F

Supervisor

Dr. ASAD WAQAR MALIK

A thesis submitted in partial fulfillment of the requirements for the degree of

MS Computer Science

In

DEPARTMENT OF COMPUTING

SCHOOL OF ELECTRICAL ENGINEERING AND COMPUTER SCIENCE

NATIONAL UNIVERSITY OF SCIENCES AND TECHNOLOGY

NUST H-12, ISLAMABAD

DECEMBER, 2015

Approval

“Analysis of Fundus Images to Detect Different Abnormalities Related to Hypertensive Retinopathy” submitted by Muhammad Ahmad have been found satisfactory for the requirement of the degree.

Advisor: Dr. Asad Waqar Malik

Signature: _____

Signature of Student

Muhammad Ahmad

NUST201362749MSEEC61313F

Copyright Statement

I hereby declare that this submission is my own work and to the best of my knowledge it contains no materials previously published or written by another person, nor material which to a substantial extent has been accepted for the award of any degree or diploma at NUST SEECS or at any other educational institute, except where due acknowledgement has been made in the thesis. Any contribution made to the research by others, with whom I have worked at NUST SEECS or elsewhere, is explicitly acknowledged in the thesis. I also declare that the intellectual content of this thesis is the product of my own work, except for the assistance from others in the project's design and conception or in style, presentation and linguistics which has been acknowledged.

Author Name: Muhammad Ahmad

Signature_____

Acknowledgements

I would like to express my immense gratitude to my supervisor Dr. Asaq Waqar Malik, who has guided and supported me throughout my thesis work and allow me to work in my own way and polish my skills. His mentorship was predominant in sustaining versatile experience in my long term career goals. I would also like to thank my committee members, Dr. Anis Ur Rehman, Dr. Asad Anwar Butt and Dr. Usman Akram who continuously guided me in my thesis, and provided their valuable suggestions and encouragement.

Dedicated to my parents, teachers and all the way special friends.

Table of Contents

Approval.....	ii
Copyright Statement	iii
Acknowledgements	iv
Table of Contents.....	vi
List of Figures	viii
List of Tables.....	x
Abstract	xi
CHAPTER 1: INTRODUCTION.....	13
1.1 Problem Statement	13
1.2 Thesis structure	17
CHAPTER 2: Medical definitions and discoveries of Hypertensive Retinopathy	19
2.1 Fundus Imaging Techniques	19
2.1.1 Fundus Camera	19
2.2 Clinical Findings	20
4) Papilledema	28
5) Causes of papilledema	29
2.3 Hypertensive Retinopathy Grading	29
CHAPTER NO 3: Literature Survey.....	32
3.1 Pre-processing of Fundus Retinal Images	32
3.2 Vessel Segmentation	32
3.3 Detection of Optic Disk (OD)	33
3.4 Retinal Vessels Classification	34
3.5 Vessels width estimation and calculation of AVR	35
3.6 Papilledema or Optic Disk Swelling	35
CHAPTER 4: PROPOSED METHODOLOGY.....	37
4.1 Pre-Processing.....	38
4.1.1 Background Removal	38
4.1.2 Removal of Noise	39
4.2 Vessel Extraction	40
4.2.1 Segmentation of Vessels using 2-Dimensional Gabor Wavelet.....	41
4.3 Optic Disk Detection.....	46
4.3.1 Optic Disk position detection.....	46
4.4 Identification of Analysis Zone.....	47
4.5 Vessels classification into arteries and veins.....	50
4.5.1 Feature Extraction.....	50
4.5.2 Feature Selection	53

4.6	Width measurement and AVR calculation	55
4.7	Detection and classification of Papilledema	57
4.8	Classification by Support Vector Machine	62
CHAPTER 5: EXPERIMENTAL RESULTS.....		63
5.1	Datasets	63
5.2	Results.....	64
5.2.1	Vessel Classification Results	64
5.3	Papilledema Detection	67
CHAPTER 6: CONCLUSION AND FUTURE WORK		68
6.1	Conclusions.....	68
6.2	Contributions.....	69
6.3	Future work recommendations.....	69
6.3.1	Detection of abnormal occlusion of vessels.....	69
6.3.2	Tele screening System for HR	69
References		70

List of Figures

Fig 1.1: Flow Diagram for calculation of AVR	11
Fig 1.2: Flow Diagram for papilledema	12
Fig 2.1: A fundus image of healthy eye, (a) Retinal Fovea, (b) Optic Disk.....	15
Fig 2.2: Normal retinal fundus image with papilla, optic cup, macula, fovea, artery and vein pointed.....	15
Fig 2.3: Generalized Arteriolar Narrowing.....	16
Fig 2.4: Image presenting Focal Arteriolar Narrowing	17
Fig 2.5: Widening of arteriolar light reflex in arteries	17
Fig 2.6: Copper wiring.....	18
Fig 2.7: Broadening effect of Arteriolar light reflex. (1). Generalized arteriolar narrowing. (2). Increase in Light reflex. (3). Copper wiring. (4). Silver wiring.....	18
Fig 2.8: Arteriovenous Nipping in retinal image.....	19
Fig 2.9: Salus's Sign, Vein converged from its original path	20
Fig 2.10: Normal tortuosity	20
Fig 2.11: Shows Worst Case Vessel Tortuosity	21
Fig 2.12: Retinal hemorrhage lesions shown in circle	21
Fig 2.13: Hard exudates placing in retina.....	22
Fig 2.14: Soft-Exudates (CWS).....	22
Fig 2.15: a) Original Image b) Papilledema Grade 1 c) Papilledema Grade 2 d) Papilledema Grade 3 e) Papilledema Grade 4.....	23
Fig 4.1: Flow chart for AVR calculation.....	32
Fig 4.2: (a). Retinal fundus image, (b). Background Mask in Binary scale.....	34
Fig 4.3: (a). Green band of fundus image and enhanced image	34
Fig 4.4: Red, green and blue band of RGB image with original colored image.....	35
Fig 4.5: a) a) Waterfall plot of for 2-D Gaussian and complex exponential	36
Fig 4.6: (a) Green and inverted green channel images	36
Fig 4.7: Different orientations for Gabor Filter	37
Fig 4.8: Gabor wavelet used for image enhancement using different scales 2, 10	38
Fig 4.9: Enflamed vessels in enhanced image.....	38
Fig 4.10: Showing low frequency response of vessels	39
Fig 4.11: a) Enhanced vascular network in image b) Binary image after thresholding.....	39
Fig 4.12: a) Retinal color image, (b) vessels in binary image, c) Vessels segmented image imposed on retinal image.....	40
Fig 4.13: a) All three channels of RGB color-space	41
Fig 4.14: a) Retinal fundus image, (b) Red band of RGB image, (c) filtered image, d) OD position indication.....	41
Fig 4.15: RGB image along with the different intensity values of the same vessel	42
Fig 4.16: Vascular Structure in retinal image	43
Fig 4.17: a) Retinal image, small vessels formed on retina are pointed	43
Fig 4.18: (a) OD position and center detection, b) OD region of interest marked.....	44
Fig 4.19a: Retinal image with centerline pixels of a vessel segment.....	45
Fig 4.19b: Retinal image with horizontal profile based features of a vessel segment.....	45

Fig 4.20: a). Intensity profiles in all three channels of RGB color-space.....	46
Fig 4.21: a). Intensity profile representation in Hue in HSV, b). Intensity Profile of vessels in S channel in HSV, c). Intensity Profile of artery and vein in V channel	47
Fig 4.22: a). In C- channel the intensity profile of vessels b). Intensity Profile in M channel in CMYK color-space, c). Intensity Profile of both type of vessels in Y channel.....	47
Fig 4.23: a). Intensity Profile in L channel of LAB color-space, b). Intensity Profile a* channel of LAB, c). Intensity Profile of B channel of LAB.....	47
Fig 4.24: Top Five Selected Features in Box Plot Representation.....	49
Fig 4.25: Vessel Width Estimation, a). Retinal binary segmented image, b). Complement of image a), c). Distance values of vessel pixels, d). One pixel wide vessels binary image, e). Multiplied image of (c) and (d)	50
Fig 4.26: Flow chart for papilledema detection.....	52
Fig 4.27: (a) Green band image of retina, (b) Resulting image after filtration	53
Fig 4.28: a) Enhanced image b) Segmented Image	54
Fig 4.29: Optic disk margin is selected from the center of OD for different grade of papilledema.....	55
Fig 5.1: INSPIRE-AVR database images.....	57
Fig 5.2: Images from AFIO database.....	58
Fig 5.3: Original image with classified image representing vessels as arteries as red and vein as blue.....	59

List of Tables

Table 2.1: KWB's Grading System	24
Table 2.2: Scheie Grading System	25
Table 2.3: Wong and Mitchel's Grading	25
Table 4.1: Parameters used for Gabor Wavelet	38
Table 4.2: Wilcoxon test results of features with p-value	48
Table 4.3: The Modified Frise'n Scale	51
Table 5.1: Datasets with annotated data by the ophthalmologists.	58
Table 5.2: Performance measures with values	60
Table 5.3: Comparison with the previous systems Using VICAVR dataset	60
Table 5.4: Comparison with previous systems	60
Table 5.5: Dataset Specifications	61
Table 5.6: Papilledema Detection Results Confusion matrix	61
Table 5.7: Papilledema Detection Results	62

Abstract

This thesis includes research related to analysis of retina to detect and diagnose the Hypertensive Retinopathy (HR), an eye disease, through fundus images. Hypertension can be observed in blood pressure in the form of high blood pressure and it affects the vasculature structure of the human body and retina as well which is mentioned by HR. This disease further leads to other major problems of human body as blindness, heart and brain diseases and strokes, if does not diagnose at earlier stages.

The automatic image analysis very important step to detect and diagnose the disease in short time with less ophthalmologic resources. The advancement in this field has made it easy and possible to detect and diagnose the HR in retinal fundus images at early stages. Before it, it was really difficult and time consuming for the health experts and ophthalmologist to observe and analyze the every image of patient to detect the signs of HR. So, it was an hour of need to develop and assemble such a tool which help the health experts to find out the clinical signs and categories the severity of HR. Initially signs appear in retinal vessels which shows the existence of HR. There are many other changes observed along with vascular changes like papilledema or Optic Disk Swelling. At advance stage of HR, Papilledema can also be observed in retina. That's why to analyze and detect the main vascular changes along with papilledema, we need some system which calculates the changes in vessels and also detects the optic disk swelling in retina. We can also evaluates the severity and presence of HR by the measurement of Arterio-Venous ratio. And basically this is the ratio of retinal arteries width to veins width. For the automatic detection of HR, CAD (Computer Aided System) has been designed. And this automated system measures the AVR by separating the retinal vessels into two types and detects the grades of papilledema. This automated system is consisted on three main steps; first preprocessing, classification of vessels and calculation of AVR and detection of papilledema, and HR grading depending on arterio-venous ratio and OD swelling. This system helps health specialists for examining and diagnosing of disease. This system obtains 87.27% accuracy on correct vessel classification and 84% on AVR calculation.

Key Words: *Vessel Classification, Fundus images (FI), Hypertensive Retinopathy (HR), Arterio-Venous Ratio (AVR), Papilledema (PE), Optic Disk (OD), Support Vector Machine (SVM), and Region of analysis (ROA), Computer-Aided Diagnostic system (CADS).*

CHAPTER 1: INTRODUCTION

Hypertension (disease with systolic blood pressure) exhibits in several customs in the body of human being. Main human body parts i.e heart, kidneys, brain and eyes are usually affected by hypertension. Arterial Hypertension affects the arteries mainly and causes damage. Actually vessels, especially arteries are flexible and elastic but due to hypertension it becomes thick and hard which causes the resistance in flow of blood and damage of vessels. We can observe this changes in vascular network of retina, thus it is called hypertensive retinopathy. That's why it is considered close to the hypertension. This disease causes the vision loss so its treatment at early stages is necessary.

Hypertension and hypertensive retinopathy can be assessed through probing the retina in fundus images. Fundus imaging is a productive way as cost-efficient and non-offensive for the health to scrutinize the flow and movement of blood in retinal vessels. It's necessary to declare here that retina of eye is the only part where change in vessels can be detected. This retinal property makes eye worthy to for analysis.

The presence of this disease can be identified and examine through clinical signs which is very important to health professionals and patients as well. It is very time consuming and painful job for doctors to analyze the each patient and identify the clinical sign for the disease. For that, many researchers have been developing some automated systems that identify the signs and weigh them conferring to the rigorousness.

With the help of such a system if developed, the health professionals can focus to cure the patient except to wasting the most of time on evaluating the clinical sign by themselves. An automated system is very beneficial for analyzing purposes especially when there is mass-screening going on.

1.1 Problem Statement

Hypertensive retinopathy is the disease which has notable effects on people worldwide. There is great need to develop an automated competent system which would help doctors for the authentic assessment of Hypertensive Retinopathy. Pakistan is such a country which owns low doctor to patient ratio. It is more difficult for the ophthalmologists to diagnose the disease if the images to analyze are very large in number and even harder when the quality of fundus

images is lower and rough. Retinal vessels have significant influence in observation and analysis of the disease, though, it becomes more difficult to segment and classify the vessels when it becomes darker in fringe areas, and worse in case of low quality images. That's why it is essential to have an automated system for analyses of retinal images which will cut down the burden of ophthalmologists which results in increase the diagnostic performance [2]. This thesis research has been done to develop an automated system which has such energy to compete the necessary requirements of ophthalmologists and patients as well. This research attempts to decrease the vision loss chances and other damages to retina with the development of this system.

1.2 Thesis scope and respected aims

The main purpose of this research is to build an automated computer aided system which diagnose and grade the Hypertensive retinopathy by estimating AVR and detecting the optic disk swelling in digital fundus retinal images. This system also grades the severity of the disease as well as detects the disease. Hypertensive Retinopathy (HR), auspiciously, is a revocable disease, that's why the basic purpose of this thesis is to build a system which can diagnose and treat the disease well.

Different anomalies and defects related to hypertensive retinopathy have to be evaluated individually so analyze the influence of every one. There are some steps performed to develop such a system.

Primarily, the fundus retinal image is pre-processed to overcome the low quality of image which includes contrast inconsistency and local brightness. This is necessary because during image attaining procedure, image is un-equally illuminated. Image enhancement and boosting is very significant step because all next steps are dependent on the image quality and satisfaction. This enlightenment also affect the analyzing process of image as it is difficult to point out the features like vascular network, drusens, exudates, papilledema and cotton wool spots (CWS) in a non-uniformly enlighten image.

The retinal vascular network is also recognized and mined next. The extraction and segmentation of retinal vascular network is as difficult as like estimation and calculation of AVR, and assessment of stages of HR is supplementary dependent upon accurate identification of vascular structure and segmentation of optic disk. In order to eliminate the vascular network

from fundus images to detect optic disk diameters to detect the papilledema, still it is necessary to accurately detect and classify the vessels to calculate the arterio-venous ratio. The position and radii of retinal vessels is also calculated.

Next, the identification and extraction of optic disk is to be done. It has an absolute significance to detect the optic disk in fundus image analysis because all vessels of vascular network initialize from it. It also give us space to identify the region of interest (ROI).

After that, the extracted vessels are categorized into arteries and veins. Accurate division of vessels is confirmed, as hypertensive retinopathy damages both type of vessels separately. The changes in vessels (arteries and veins) cannot be examined without differentiating the vessels. The next step of this method is related to the detection of Optic disk and analyze the OD swelling which indicates the severe phase of hypertensive retinopathy. So, health professionals will be assisted by this system to categorize the severity of HR.

Finally the AVR is estimated and analysis of hypertensive retinopathy grades from calculated AVR and detection of stage of papilledema. Flow diagrams of proposed methods for calculation of arterio-venous ration (AVR) and existence of papilledema are shown in Fig 1.01 and 1.02 respectively.

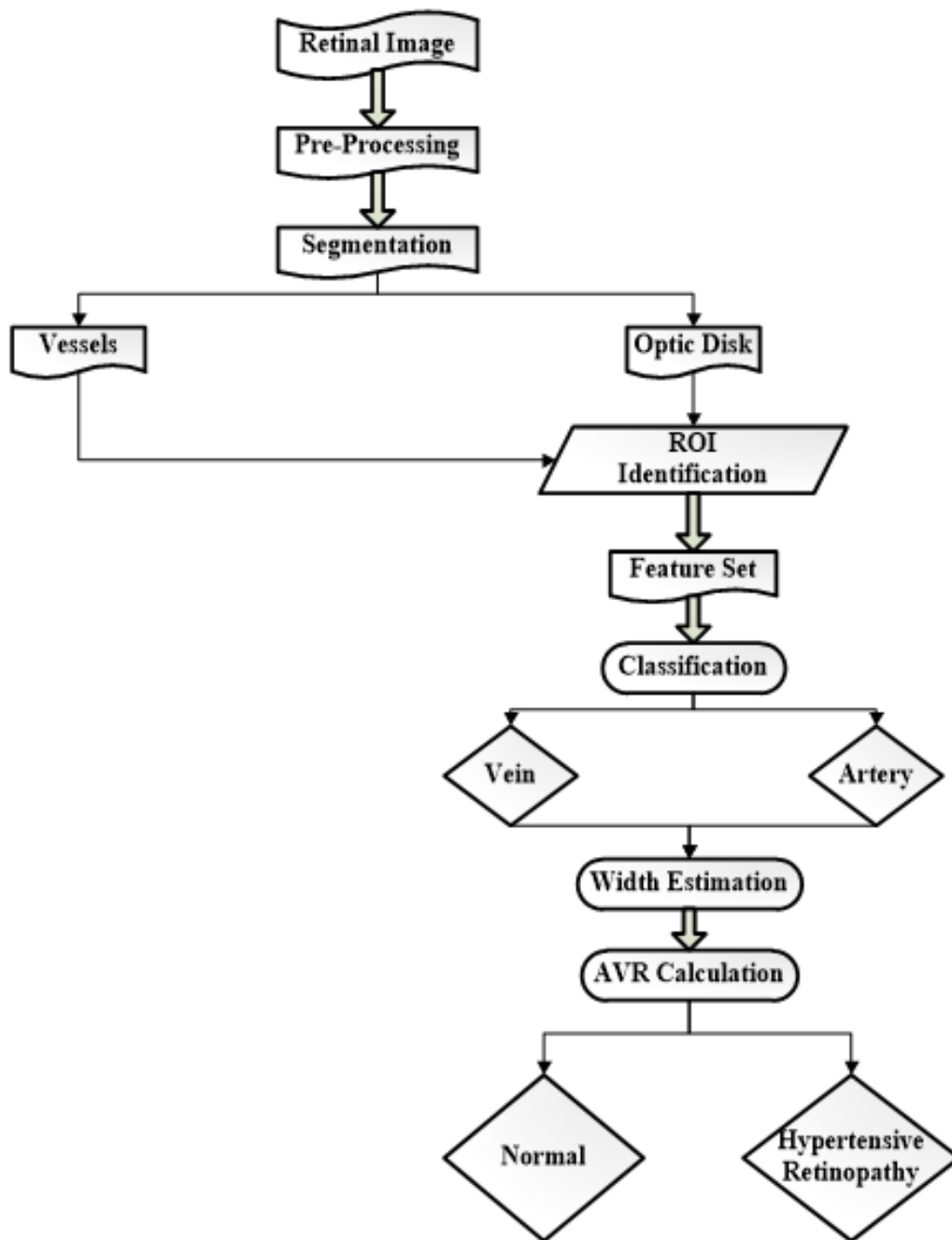


Fig 1.01: Flow Diagram for calculation of AVR

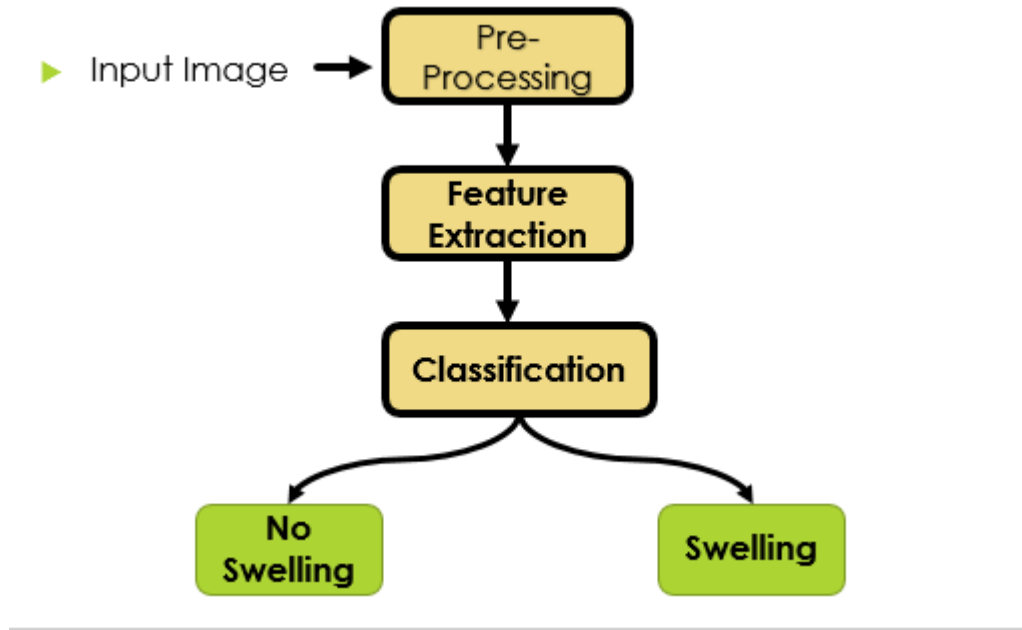


Fig 1.2: Flow Diagram for papilledema

1.2 Thesis structure

Remaining part of the thesis is prepared as following steps and divided into chapters:

Chapter 2 of this thesis describes the HR completely and along with its different stages from the view of health professionals. The sound effects of Hypertension on human's eye and the damage happens due to this disease on vascular network and other main parts of retina are explained thoroughly in second chapter. This chapter provides an outline and overview about fundus camera and retinal fundus photography along with fundus imaging method for the observation of other retinal diseases.

Chapter 3, a literature survey of different present techniques for the detection and diagnosis of different anomalies of HR.

In the next chapter, the methodology proposed for an automated system is described. It comprises analysis of retinal fundus images using advanced image processing techniques for the classification of vessels by feature extraction using support vector machine.

The description related to databases which are used for testing and training the classifiers for the classification purposes is expressed in chapter no. 5. It includes all trials for this method

and their results and comparisons in the form of different considerations. Comparisons with other system are also explained in this chapter.

Conclusion for the proposed method and future related work is discussed in Chapter 6.

CHAPTER 2: Medical definitions and discoveries of Hypertensive Retinopathy

This second chapter includes main clinical observations for hypertensive retinopathy. These medical observations (Clinical findings) are symptoms and signs observed by a doctor when he examine the patient, in hypertensive retinopathy it correlates to the abnormalities and effects of HR exist on retinal images.

2.1 Fundus Imaging Techniques

Fundus is the inner surface opposite to the lens in the human eye. Fundus of eye is included retina, optic disk, macula, fovea and posterior pole. Creation of an image of fundus is associated with fundus photography [3]. Fundus imaging or photography is done with the help of a special fundus camera that contains a low power microscope with an attached camera [4]. We can observe the microcirculation of the blood directly and non-invasively that's why the retina of the human eye gives us a great specialty over other body parts. The flow of blood in smallest blood vessels which are exist within organ tissues is called microcirculation [5]. The change in flow of blood mostly damages the retina.

2.1.1 Fundus Camera

Fundus camera is used to take the image of fundus; the person to be examined is normally sits in front the fundus camera machine keeping his/her chin at chin rest and holding its forehead along the bar. Then the ophthalmologist presses the shutter button with a flash fire, the fundus image is created like below. These retinal photographs the used by the ophthalmologists to diagnose, follow and treat the different eye ailments [5].

Fig 2.1 and 2.2 represents the fundus images with normal conditions [6].

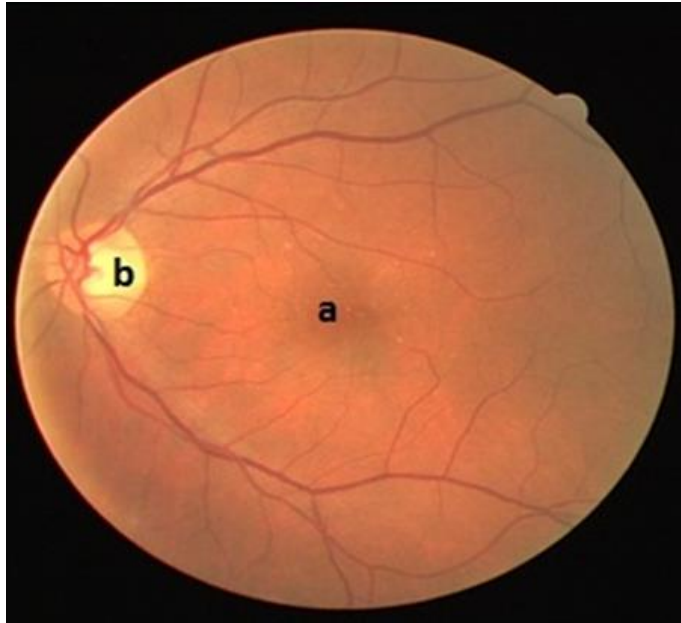


Fig 2.1: A fundus image of healthy eye, (a) retinal Fovea, (b) Optic Disk

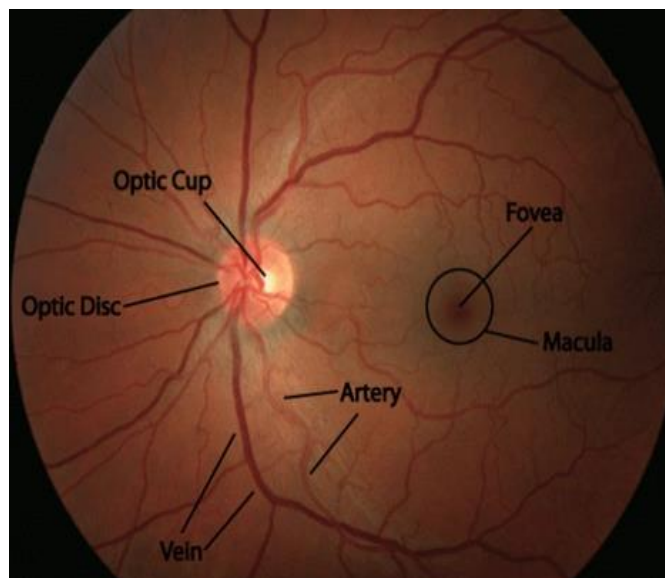


Fig 2.2: Normal retinal fundus image with papilla, optic cup, macula, fovea, artery and vein pointed [7]

2.2 Clinical Findings

Two main types of abnormalities are found on retinal images which are classified accordingly, one is called vascular changes and the other is called extravascular changes in retina. Both types of abnormalities participate to diagnose and calculate the grade of hypertensive retinopathy. In order to explain them, firstly vascular changes are represented:

a) Vascular retinal changes

1) Arteriolar Narrowing

Arteries mostly become narrow in retinal images in HR and this state is called arteriolar narrowing. There are two types of narrowing, first generalized arteriolar narrowing and the second one is focal arteriolar narrowing. High blood pressure is indicated by presence of both type of narrowing. Although generalized narrowing is associated with mild hypertensive retinopathy and focal arteriolar narrowing with severe retinopathy.

- **Generalized Arteriolar Narrowing**

Generalized arteriolar narrowing is associated with narrowing of central artery or arteriole. Hypertensive retinopathy is classified depending on how much the arteries shrunk; more it become thin more will be severe. Mostly other type of narrowing called generalized arteriolar narrowing is evaluated by calculated arterio-venous ratio AVR (ratio of width of arteries with the width of veins) [8]. The normal AVR value is compared with resultant calculation in order to Fig out the grading of hypertensive retinopathy.

Fig 2.3 shows generalized arteriolar narrowing.



Fig 2.3: Generalized Arteriolar Narrowing [8]

- **Focal Arteriolar Narrowing**

The shrinking or dilation of native regions of local arteries or major artery is called focal arteriolar narrowing. Due to this kind of contraction, the artery or arterioles become too much narrow like a thread and this state of narrowing is known as the severe stage of HR.

Fig. 2.4 shows the focal arteriolar narrowing of vessels of eye.

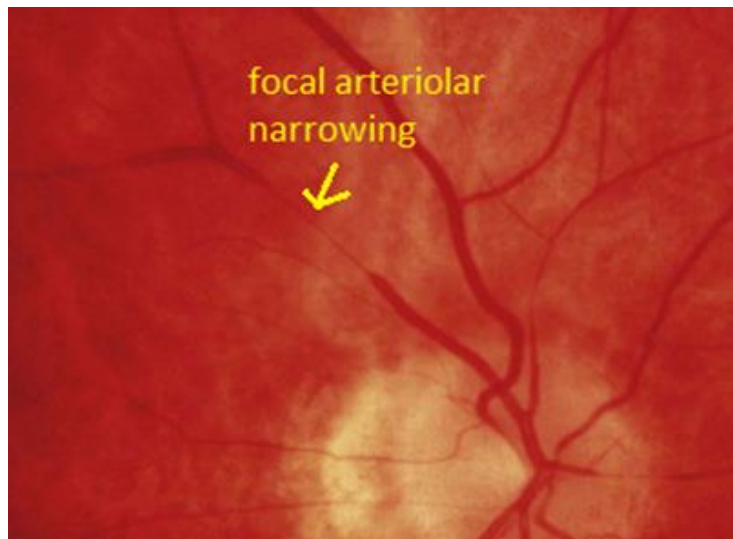


Fig. 2.4: image presenting Focal Arteriolar Narrowing [9]

2) Light reflex widening of arterioles.

In the arterioles, the arteriolar wall is not definable, only visible part is the column of red blood cells. In the middle of that blood cells column, a thin line with reflected surface can be seen which is called normal light reflex. These arteriolar walls change the form and become dark, the light reflex becomes less bright. Blood pressure is further raised by time which causes the arteriolar wall becomes thicker and results in losing of brightness in light reflex, which adopts color like copper wire or silver wire [10]. Fig. 2.5 presents broadening of light reflex. Fig 2.6 shows the copper wiring and fig. 2.7 indicates broadening of arteriolar light reflex.

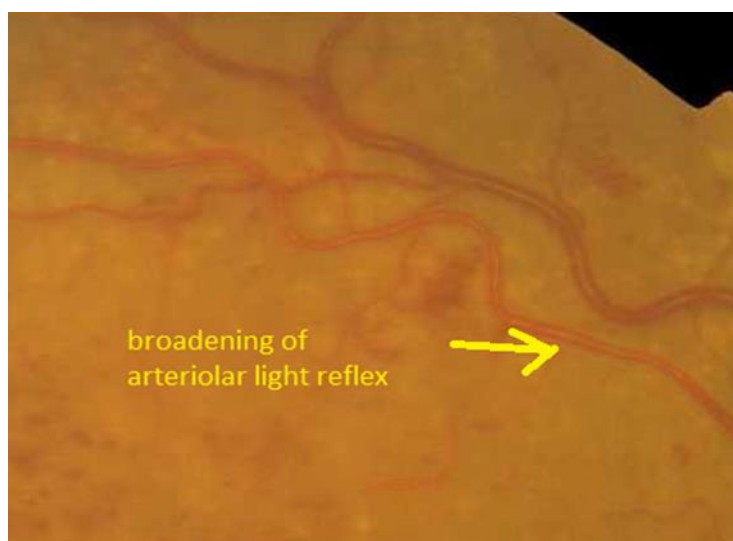


Fig. 2.5: Widening of arteriolar light reflex in arteries [10]

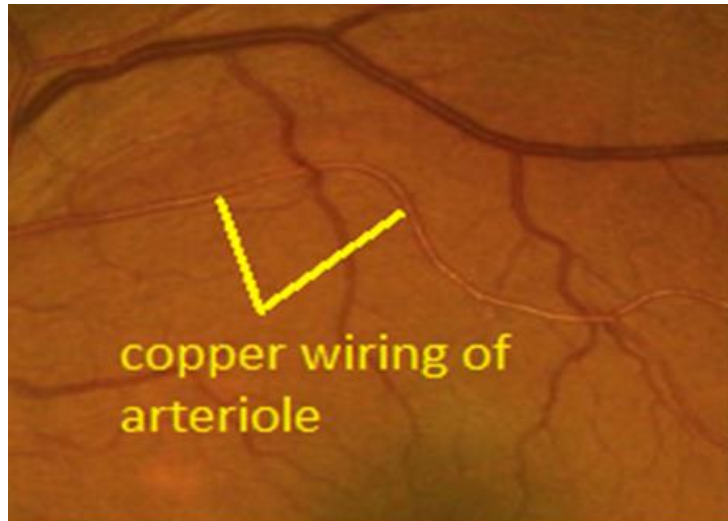


Fig. 2.6: Copper wiring [10]

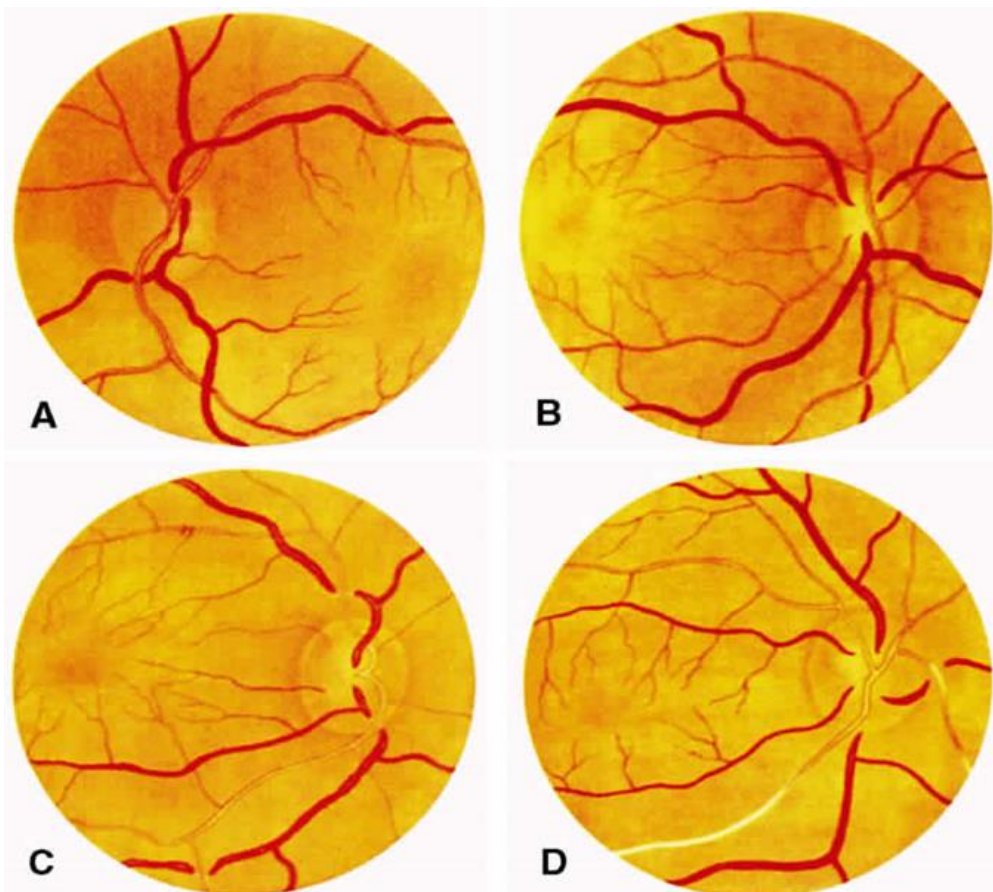


Fig. 2.7: Broadening effect of Arteriolar light reflex. (1). Generalized arteriolar narrowing. (2). Increase in Light reflex. (3). Copper wiring. (4). Silver wiring [11] [12]

3) Crossing Abnormalities

The crossing or the meeting points of vessels in retinal images are places where we can observe crossing abnormalities. The unconventionalities at the crossing points help us in the correct

grading of the hypertensive retinopathy. And the anomalies often are the result of stiffening of walls of arterioles. In the resultant, veins crossing at that points are compressed or deflected from original paths.

i. Gunn's Sign

When artery crosses the vein, at that point, the edges of veins are become thin, this condition is called gunn's sign. It's also called arteriovenous nipping. Vein can be completely depressed by the thickness of artery or partially pressed. Fig. 2.8 shows gunn's sign in retinal image.

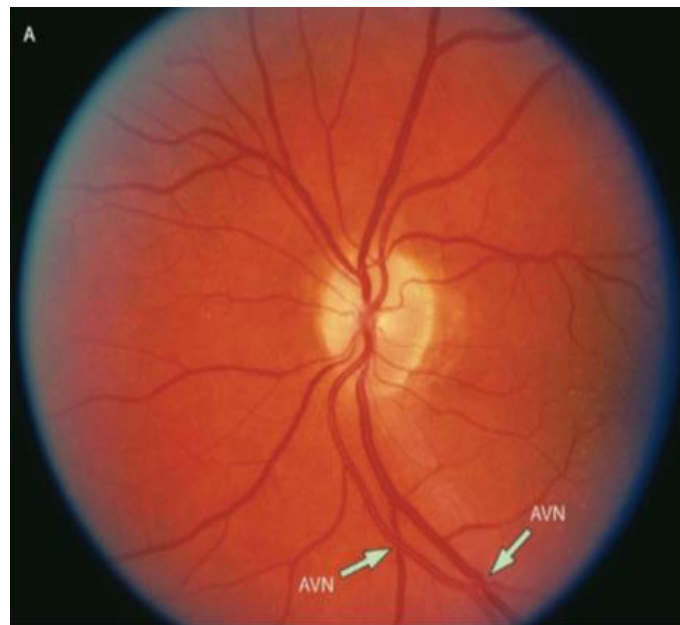


Fig. 2.8: Arteriovenous Nipping in retinal image [9]

ii. Salus's Sign

Salus's sign is associated with the path convergence of veins at the crossing point from its original course. The reason for this phenomena is also the thickening of the arteriolar walls. Due to this thickness, the vein get turn and forms a new shape like "S", which is refer to its name Salus's sign.

Fig 2.9 presents the Salus's Sign in vessels.

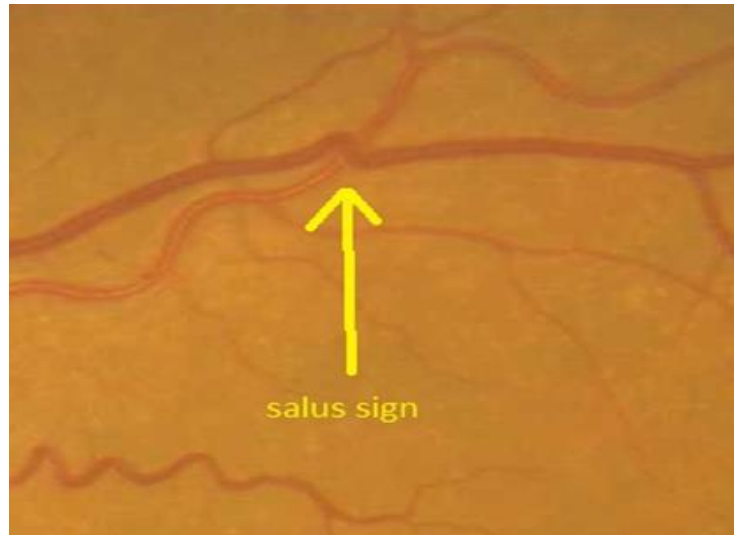


Fig. 2.9: Salus's Sign, Vein converged from its original path [13]

4) Tortuosity

Tortuosity in vessels is the re-orientation of the vessels mostly refers to the major sign of vascular abnormality [14]. This state indicates the unusual turns and twists in vessels. This abnormality often associated with arteries but in the severe state of hypertensive retinopathy, it also can be seen in veins. Two different cases of vessel tortuosity is presented in Figs 2.10 and 2.11. The first one shows normal tortuosity and the other one shows severe tortuosity [15].

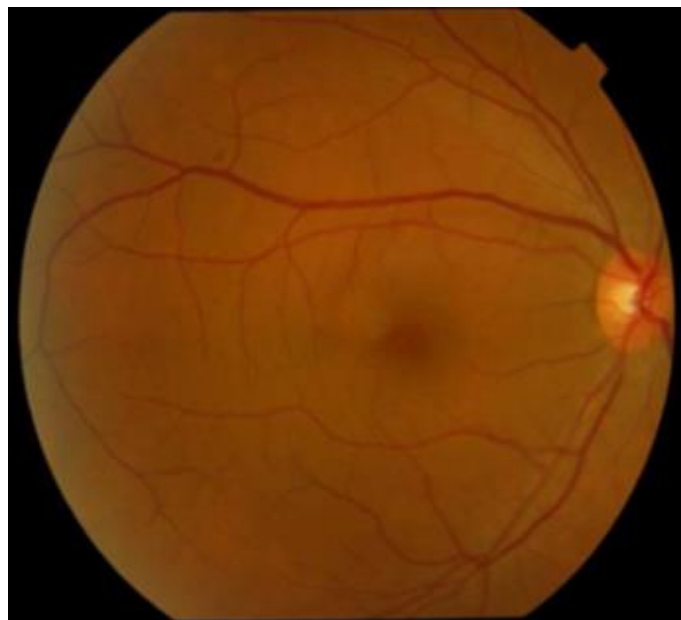


Fig. 2.10: Normal tortuosity [15]



Fig. 2.11: Shows Worst Case Vessel Tortuosity [15]

b) Extra Vascular changes

1) Retinal Hemorrhage or Lesions

Blood vessels in retina when leaked causes Retinal Hemorrhages in the eye [16]. Hypertension is one of the main reasons of this type of blood leakage and after that it becomes the sign for critical state of hypertensive retinopathy. These can be found out in different shapes in retina of the eye like flame shaped, round shape lesions etc. Fig. 2.12 presents dot hemorrhages [17].



Fig. 2.12: Retinal hemorrhage lesions shown in circle [15].

2) Hard Exudates (Yellowish Spots)

Hard exudates usually exists near the macula in the posterior pole like yellow spots [22]. Fig. 2.13 shows hard exudates in the retina of eye [17].



Fig 2.13: Hard exudates placing in retina[17]

3) Soft Exudates

Cotton wool spots also called soft exudates are the bright scratches in the retinal images. These are also sign of the severe state of hypertensive retinopathy (HR). They look like whitish bright type soft spots. Fig 2.14 shows soft exudates as CWS [17].



Fig 2.14: Soft-Exudates (CWS) [17]

4) Papilledema

Papilledema is one of the types of abnormalities of retina which relates to the very severe case of hypertensive retinopathy. This is related to optic disk. In this situation, optic disk is swollen and the size of OD is increased in retinal images as compared to the normal OD size. This type of Disk swelling is occurred when flow of axoplasmic fluid is reduced in the nerves of optic disk. Basically cerebrospinal fluid is filled inside the nerves which are opened in the brain. So the increase in pressure in those nerves is directly affects the nerve head in the optic disk and damage the flow in the exit point of nerve in the eye and it results in the optic disk swelling due to the optic nerve head swelling. It is the severe case state of the hypertensive retinopathy. Fig 2.15 shows the images with sign of Optic Disk swelling.

Papilledema is basically bilateral disease. It affects the both sides of human eyes. It is a rare case that papilledema occurs in single eye. It requires attention on urgent basis.

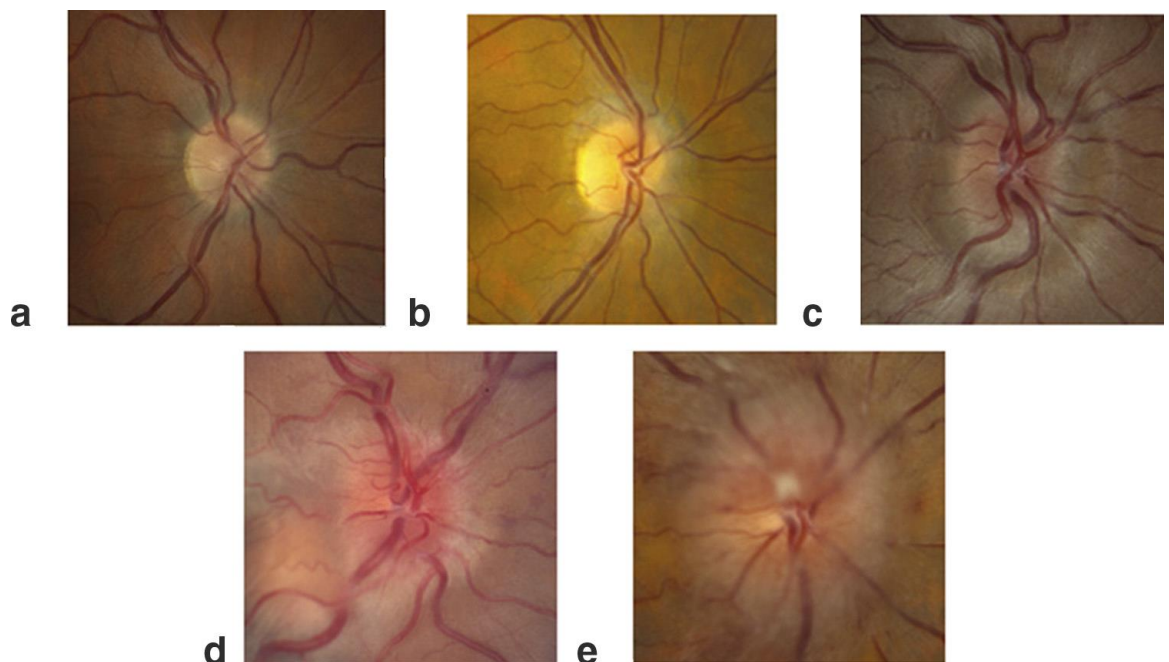


Fig 2.15. a) Original Image b) Papilledema Grade 1 c) Papilledema Grade 2 d) Papilledema Grade 3 e) Papilledema Grade 4

5) Causes of papilledema

ICP (Inter cranial pressure) is the main cause for this disease. Normal value for ICP is 250mm water level. But due to that unusual exoplasmic flow of that fluid papilledema occurs. This symptom totally depends on the increasing level of ICP. Sometimes it increases very slowly and sometimes very rapidly. In first case it takes weeks while in later case it can occurs in a day only. In hypertensive retinopathy papilledema shows the very critical and severe stage and it needs very urgent attention.

6) Signs of papilledema

There are different signs of papilledema over there like:

- Margin of OD gets blur.
- Tortuosity in veins gets notable.
- With time being disc is elevated
- Soft exudates and hemorrhages appears around the disc

2.3 Hypertensive Retinopathy Grading

To grade the hypertensive retinopathy, there are very few scales have been developed yet to analyze the severity of hypertensive retinopathy. First one was proposed by Keith, which is named as Keith Wegener Barker grading system then later Schie proposed the grading system. Wong and Mitchell also proposed another grading system [21][22].

Table 2.1: KWB's Grading System

Grade	Features
Normal	No Sign, Normal eye
Grade I	Generalized arteriolar narrowing
Grade II	Generalized and focal arteriolar narrowing, central light reflex and crossing abnormalities
Grade III	Occurrence of Soft exudates along with sign of Grade 2 and hemorrhages
Grade IV	Papilledema along with previous signs

Table 2.2: Scheie Grading System

Grades	Symptoms
--------	----------

Healthy eye	No Signs
Grade I	Very less Sign of Arteriolar Narrowing
Grade II	Generalized and focal arteriolar narrowing and central light reflex
Grade III	Copper wiring signs and arteriovenous compression
Grade IV	Silver wiring in arteries and arteriovenous crossings abnormalities

Table 2.2: Wong and Mitchel's Grading

Grade	Signs
Minor Hypertensive Retinopathy	Classified according to one or two sign stated: <ul style="list-style-type: none"> ✓ Generalized arteriolar narrowing ✓ Focal Arteriolar Narrowing ✓ Salus's Signs ✓ Arteriolar Central light reflex
Modest Hypertensive Retinopathy	Presence of one or two listed below signs <ul style="list-style-type: none"> ✓ Haemorrhages ✓ Microaneurysm ✓ Soft Exudates ✓ Hard exudates
Malicious Hypertensive retinopathy	Papilledema along with Modest HR

AVR for different steps of HR is shown in fig 2.15 [25]

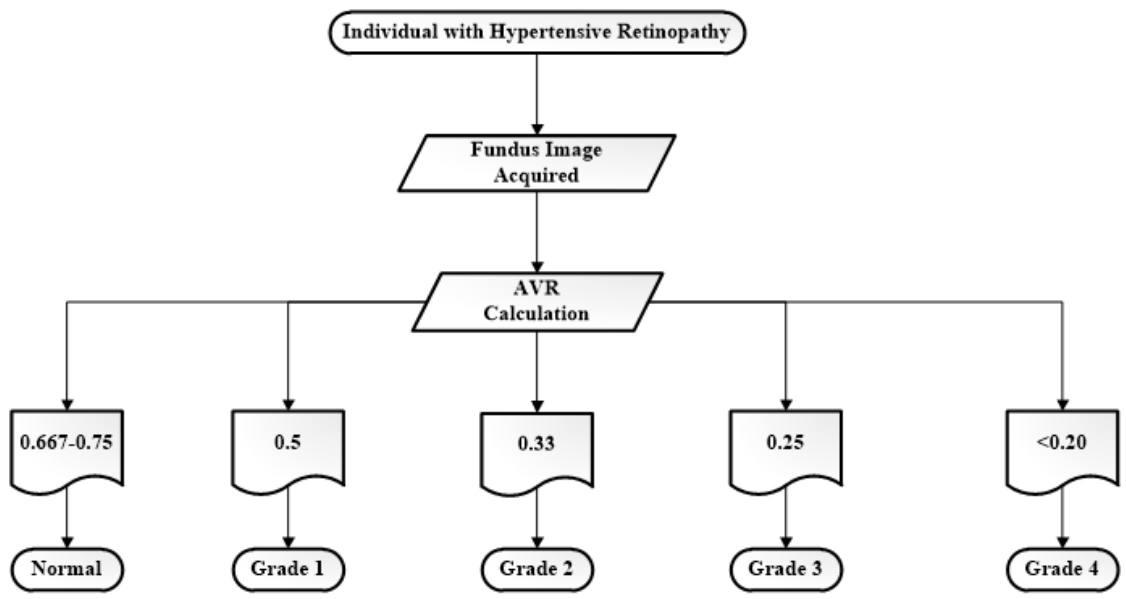


Figure 2.15: AV ratio for different grades of HR

CHAPTER NO 3: Literature Survey

Medical researchers have been working for many years to develop such an automated system which will be able to detect and diagnose the disease. These automated diagnosing system lessen the time consumption in order to help out the health experts for mass-screening, are low-cost as well. Such automated systems got much importance over the old manual screening methods revealing the benefits offered with them. At the start of the research, more or less, the method is same, adopted by every researcher. The adopted techniques and methods used in the past researches to develop a computer aided system for HR diagnosing is discussed and explained in the chapter.

3.1 Pre-processing of Fundus Retinal Images

The Retinal images mostly carrying much extra information and noise in it. To obtain a clear and better quality retinal structures, these images are pre-processed first of all. This clarity and better visual quality directly leads to better results, when these retinal images are enhanced and pre-processed. Background variability and luminosity is measured in [24], and then it compensate this variability. Dark and bright borders of the fundus images are also a different type of problem, either contained at one side of image or around the whole. These border pixels are replicating by the adjoining pixels, when this issue has been observed in [25]. These replication of the border pixels also has been served with the Gaussian filter. On the other hand, non-luminosity problem is also observed and was overwhelmed by using histogram equalization in [26] by Ortiz et al. In [27], background illumination has been compensated by using median filtering.

3.2 Vessel Segmentation

Researchers have mostly ascribed and followed two techniques in proposing the vessel segmentation algorithms. First technique, as followed, the vascular structure from retinal images is detected and segmented. Then those segmented vessels are categorized pixel-wise to obtain the more accurate segmentation results, in the second step. Different techniques were used for the vessel segmentation by the researchers. In [28], top-hat transformation is used from Morphological operations, which further combined the results of transformation with the double-ring filtered results followed by thresholding also in [28]. Gabor wavelets are used in [26] for blood vessel extraction. Centerline pixels of extracted vessels column is obtained by

Hessian Matrix, which is further summed with the results, gathered from Gabor wavelet on which Niblack thresholding algorithm is applied. A pixel-base classification of vessels is added in research by Marin et al. [29] which firstly obtain the features from the vessels and then categories them as vessel or non-vessel. Pixel-base classification is also done by [30] for vessel segmentation and they used Gabor wavelet and line operators to extract the features. This is done individually on each pixel and after that all pixels of vessels are classified as vessels or non-vessels. Shabbir et al. [31] has proposed the comparison of wavelet based segmentation and matched filter which is the comparison of the results of both approaches.

3.3 Detection of Optic Disk (OD)

Optic Disk (OD) is the other main part of the retina which contributes a lot in the development of automated system for diagnosing of the disease. Segmentation and detection of Optic disk accurate position in retinal fundus images is quite significant for the analysis. OD localization is the most important and quite necessary in many tasks like analysis of OD swelling, to find Region of Interest (ROI) for vessel classification along with the vessel segmentation, as OD is the emerging point of the all vessels. There are many proposed methods in order to detect and segment the optic disk automatically by many early researchers, some of them narrated here. A novel method for OD localization and segmentation is proposed by H.YU et al. [32]. Template-matching method is used to detect all candidate regions for OD, and then vessel – pattern property inside OD is used to select the correct candidate region, thus it's the correct candidate region which leads to segmentation of OD boundary in retinal preprocessed image which is found with the help of local gradient information. MESSIDOR, a publically available dataset, is used to test the above described method which has achieved the great 99% accuracy. Some of the researchers have used morphological operations as well. Among all of them some researchers got some noteworthy results like [33] and [34]. Closing and opening morphological operations are applied on the located OD position through shade-correction in the first paper. These shade correction technique is applied on original RGB image. In the latter one, researchers have located using brightest region method with use of LoG filtering. This group of researchers also proposed method in which they have used Hough transform for more accurate boundary location in [35] and also the same group in their recent research [36] proposed a new method for OD localization which employs vessel-contrast along with template-matching property. And this method was tested on DRIVE dataset which had yielded specificity and sensitivity 67% and 83% accordingly.

3.4 Retinal Vessels Classification

In the last few years, some of researches have gained notable significance in the eye of world researchers. Automatic blood vessel classification in fundus retinal images is became one of those significant researches and it has proved yet. Many semi and fully automatic systems have been proposed. Important of them will be discussed next. Murmatsu et al. used vessel centerline pixels to extract color features and then categorized the vessel segments depending upon these features. This method was tested on publically available dataset DRIVE and it produced the results with 75% accuracy. As like this, [25] has also used centerline features but no other feature along with the profiles across the vessel segments but classification was done with only centerline pixels. A group of researchers proposed a new technique for vessel classification basis on the division of retinal image into four quadrants and then rotate the axis through 20° between 0° and 180° . Further, they classified the feature vector using K-mean clustering obtained from vessel segmentation in each overlapping region. Finally all results from each individual region is combined and then again classified. This technique is applied on a local database of 86 retinal images. G.Mirsharif et al. [38] has proposed the methodology with the slight alteration in the mining of features from centerline pixels as they used the group of 18 consecutive pixels after implementing different size of pixels length, then took mean of these features and classify the vessels. They had also used the DRIVE database and accuracy attained was 86%. In [39], retinal vessel classification was done by feature vector which was formed by two different approaches pixel-based and profile-based. Both approaches were messing with the color features of the pixel values. First pixel-based feature vectors are prepared using mode of the values of the whole component and the value of different color channels of the pixel and on the other hand the profile-based feature vectors were prepared through measuring the median and mean of the color in the profile. Further they also used the unsupervised k-means clustering algorithm to categorize the vessels into veins and arteries. Probability of the feature vector was also the key point in the classification of feature vectors because the vessels were also classified multiple times deu to the overlapping regions. Only vessel having highest probability among all was labeled, against the mean of all probabilities. Sensitivity for arteries and veins of these images is 0.7819 and 0.8790 as per order. Red channel has significance in RGB colors due to having more intensity in arteries than veins, thus, it was nominated. On the basis of mean intensity of red channel, researchers in [26] had done the classification. The higher the mean intensity of components are classified into arteries and the ones with lower values are grouped into veins class as well. Arteries achieved higher accuracy with 82% against

veins with 50% in the evaluation after testing this technique on 15 retinal images. Relan et al. has proposed a method in [40] for the classification and tested on the VAMPIRE dataset. They have classified the vessels on the bases of color illumination. The four basic features were clearly identified as Mean of red (MR), Mean of green (MG), Mean of hue (MH) and Variance of red (VR). This classification was purely executed on two quadrants from total four quadrants, at the same time.

3.5 Vessels width estimation and calculation of AVR

The vessel estimation and its width measurement has not got the much focus by the researchers till. Semi-automatic techniques are still used by the researchers for the width measurement. Some described the methods to measure the blood vessels like Ortiz [26] by extracting the vessel borderline and vessel structure. They calculated the displacement perpendicular to vessel boundary. In [41], they proposed a method to calculate width by using centerline pixels and boundary pixels.

3.6 Papilledema or Optic Disk Swelling

There is not major contribution of research already done by the researcher for papilledema in fundus imaging. Most of researchers used OCT or any other type of images to detect and diagnose the papilledema therefore research phase in fundus images does not contain much information. In [58] the research group used color fundus images and detect the papilledema by calculating the optic disk volume which is a measuring tool of detection of papilledema. They have used total 29 fundus images for testing the algorithm which were considered with optic nerve head. OCT 3-D images were also used for the 3-D nerve head estimation. For OCT images an automated algorithm was used. Frisen scale was used to grade the papilledema for the effected fundus images. Comparison of color fundus images and OCT 3-D images were used to obtain the better grading result of papilledema. In another research [57] the group of researchers had used fundus images to classify manually by the ophthalmologists but OCT images were used to detect the papilledema by measuring the variabilities in retinal nerve fiber layer thickness with respect to the RNFL of healthy eyes and eyes with mild papilledema. These images were scanned in circle to detect the variation in diameter of the optic disk. They

have used 41 images to test the results. They found 17 normal people without any sign of papilledema while 15 with mild papilledema and 5 with other type of papilledema called pseudo papilledema.

CHAPTER 4: PROPOSED METHODOLOGY

This chapter includes proposed methodology in detail. All the steps are completely described here in this chapter. These steps consist of many approaches which are almost similar but different in single step. Which step is most useful in this methodology is difficult to find out. A need is existed to analyze the each part of this methodology to carry out the best part of the whole technique [2].

The main focus of this approach is to classify the retinal vessels with much improvement for correct detection of hypertensive retinopathy. This is the back bone of this whole process to correctly classify the vessels into veins and arteries as this disease is fully depends upon the accurate calculation of arterio-venous ratio which can be measured in full health after correctly classification of retinal blood vessels.

There are many irregularities and disorders related to Hypertensive Retinopathy and thus there is necessary to analyze each of the abnormality in isolation by evaluating the effect of each on of them. Many steps are to be executed for the development of an automated system for such abnormalities. These performed steps of proposed method are; background and noise removal as preprocessing of the fundus images, extraction and segmentation of vessels as well as optic disk, determination of region of interest, categorization of retinal vessels into arteries and veins, calculation of AVR for classified vessels, detection of papilledema and grading of HR into different stages.

Fig 4.1 shows the complete Fig of proposed method.

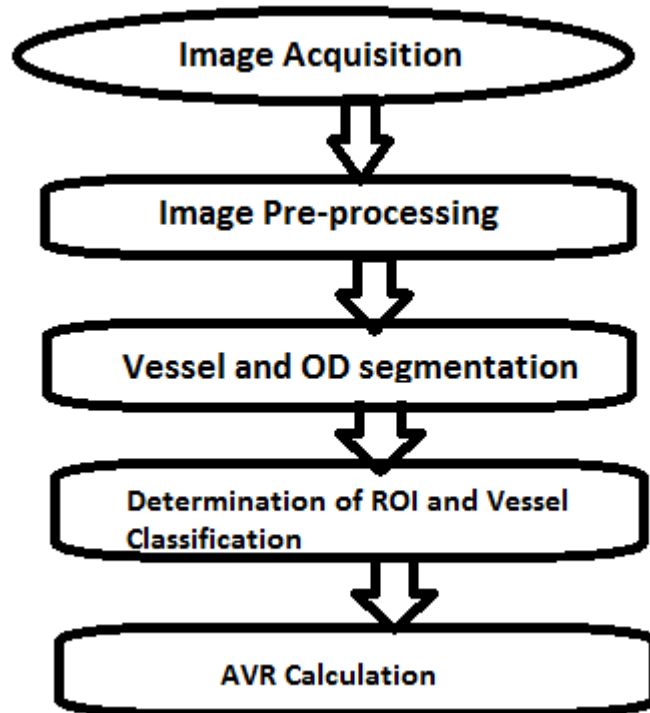


Fig 4.1: flow chart for AVR calculation

4.1 Pre-Processing

In the beginning of this step, retinal fundus image is preprocessed for the reparation of quality impurity due to variability of contrast and lightness, and addition of local luminosity. This step is performed due to non-constant illumination at the time of image acquirement. Image is enhanced at this step as it is very important to have good quality image for the next oncoming steps. The effects of HR maybe find difficult to detect as if there is illumination is involved which further disturbs the diagnostics process [1].

On the other hand of this illuminations, there is also necessary to get the main concerned area of the retinal image and the other background area should be separated. This foreground area mainly adds up on main parts of the retina. Noise removal is also performed before the image enhancement.

4.1.1 Background Removal

The retinal fundus image acquired by the camera is consists of two parts; one is circular foreground and black color background. Actually this background is not completely black and comprises much noise in it, that's why it is preferred to measure and remove this background.

Without removal of background, the results of this process could be changed due to the addition of noisy pixels in this process. The foreground are is only to be analyzed in the process of feature extraction and sign detection. This shows the importance of background pixels removal. In the pre-processing, first of all background estimation is performed using different methods based on mean and variance [27]. These mean and variance based methods are applied which leads to form a binary background mask. Actually this mean based method works out in each sub-block of image locally. So this method is applied to retinal images. And it yields much better results in comparison of global methods [27]. These steps are listed below which are involved in background segmentation using following steps:

- Initially retinal image $I_m(i, j)$ is divided into b size blocks of non-overlapping position.
- $M(I_m)$ represents the local mean of each block by using following equation 4.1.

$$M(I_m) = \frac{1}{b^2} \sum_{i=-\frac{b}{2}}^{\frac{b}{2}} \sum_{j=-\frac{b}{2}}^{\frac{b}{2}} I_m(i, j) \quad 4.1$$

- This local mean is used to calculate the standard deviation $S(I_m)$ using equation 4.2.

$$std(I_m) = \sqrt{\frac{1}{b^2} \sum_{i=-\frac{b}{2}}^{\frac{b}{2}} \sum_{j=-\frac{b}{2}}^{\frac{b}{2}} (I_m(i, j) - M(I_m))^2} \quad 4.2$$

- Thresholding is applied by choosing a value which describes that a block is related to foreground or background. If the obtained value after applying standard deviation is larger than the thresholding value then it is consider as the part of foreground of image otherwise it is considered as the background or black area of image [27].

4.1.2 Removal of Noise

The marginal areas of the retina which lies in distance from optic disk are offers more darkness and ambiguity. Noise as noisy pixels of retina are also an issue. This noise removal and quality improvement in marginal areas are done using histogram equalization. And further this resultant image is filtered out through median filter [27].

This noise removal and quality enhancement steps are carried out because in the next steps it is necessary to have an improved image i.e. vessel extraction and segmentation. Original image along its background mask is shown in fig 4.2. Original image in green channel of RGB and equalized image after applying median filter is shown in fig 4.3.

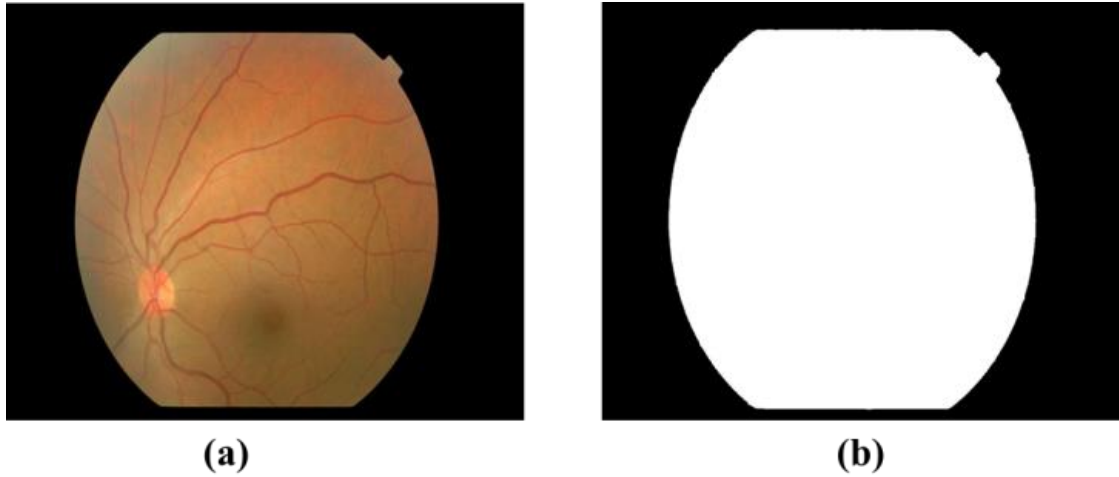


Fig 4.2 (a). Retinal fundus image, (b). Background Mask in Binary scale

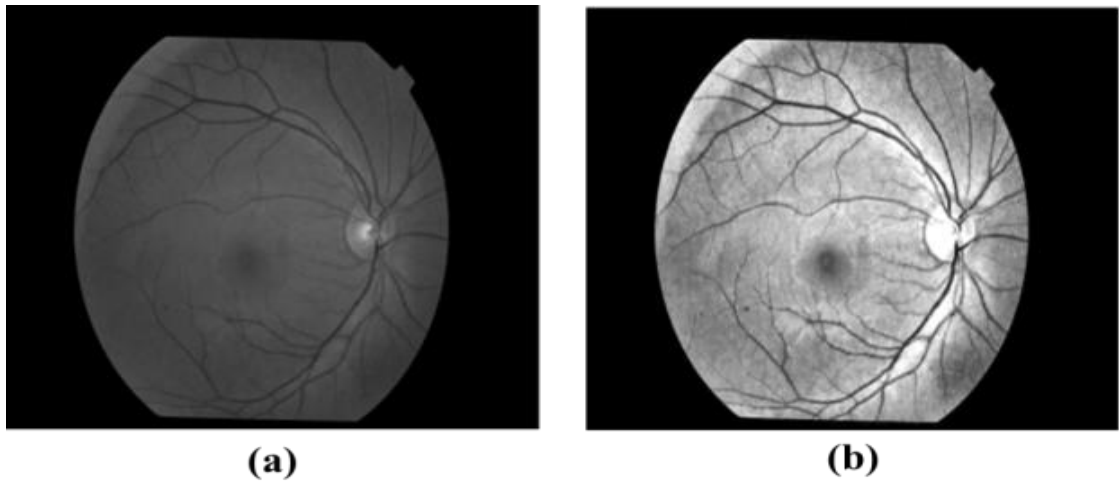


Fig 4.3 (a) Green band image with filtered image

4.2 Vessel Extraction

Vessel identification and extraction is done after the enhancement of vessels in retinal image. This step is the most important step of the methodology as the AVR calculation is fully dependent on the extraction of vessels and as the true grading of HR is evaluated by the correct classification of the vessels. Even, in order to detect the papilledema, the extraction of vessels is also necessary to detect the border of optic disk and to exclude the vessels.

The original retinal fundus image is existed in RGB color-space. The red channel of it, is already saturated while the blue channel is found empty so that the green channel is considered. This band of RGB represents the true path of vascular network and the other nominated parts of the retina. In the inverse of green channel the vessels becomes lighter than the other

background of the image. So, the green channel of the image is selected for the vessel extraction. All the three channels are shown below in fig 4.4 respectively. This Fig best presents the vessels in green channel.

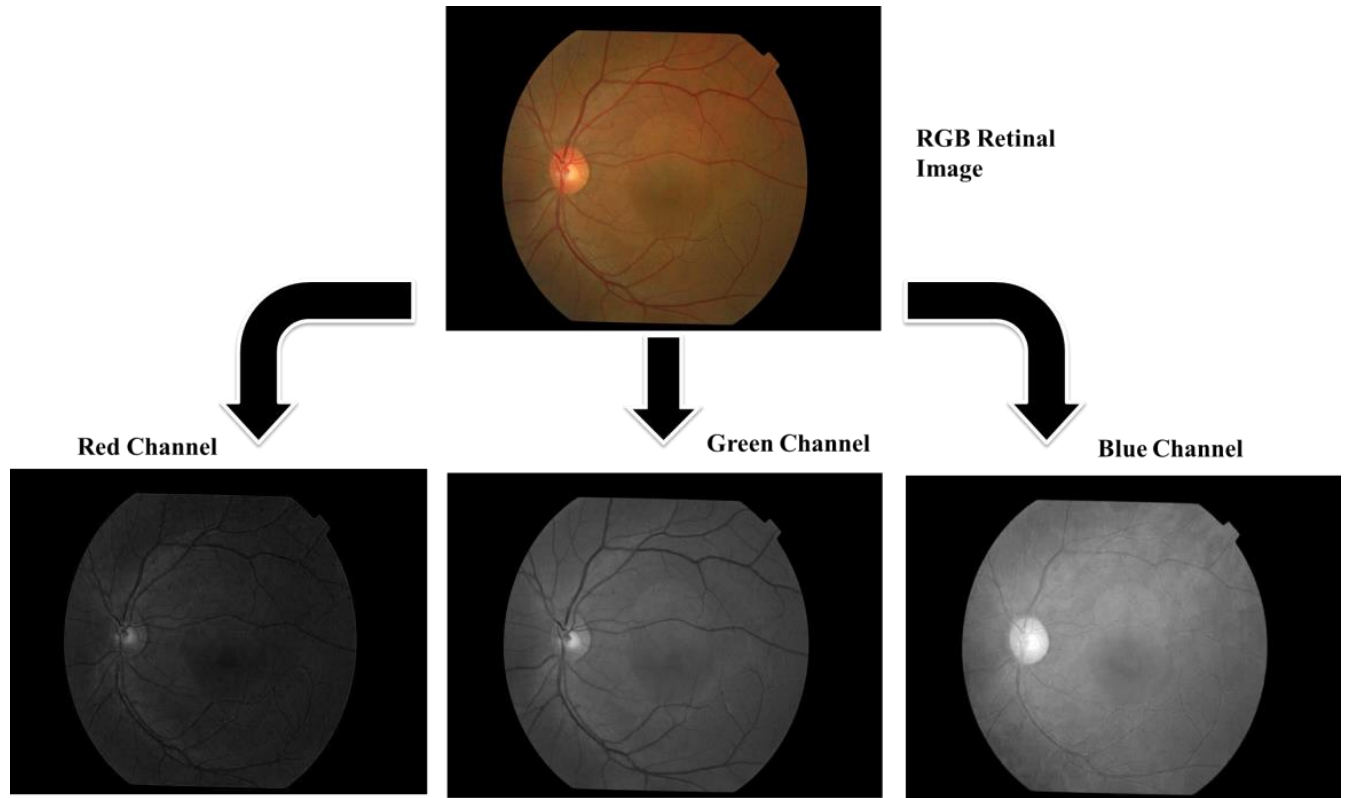


Fig 4.4 Red, green and blue band of RGB image with original colored image

4.2.1 Segmentation of Vessels using 2-Dimensional Gabor Wavelet

Vessels are segmented by another technique which is called 2-D Gabor wavelet. This filter bank is consist of different filters with specific orientation and scales. Whenever the orientation of the filter matches with the texture pattern and direction of the image, it generates a high response in result. So, these filters helps out in the analysis of direction of texture part in image [42]. Frequencies localization and detection is done through scale of filters. High frequencies deviations are enhanced when the scale is low while low frequencies are enhanced when the scale is high. The low scale helps out to detect the fast changes and high scale shows the slow changes in frequencies. As the retinal images contained the directional arrangements that's why the Gabor filter helps in enhancement of the vessels in the image by its ability to highlighting the directional pattern.

This filter bank is in actual a grouping of 2-D Gaussian and complex exponential sinusoidal.

Below is the equation showing the Gabor wavelet [26].

Fig 4.5 shows Waterfall 3D plot of Complex exponential and 2-D Gaussian.

$$G(x, y) = \frac{1}{2\pi\sigma\beta} e^{-\pi\left[\frac{(x-x_0)^2}{\sigma^2} + \frac{(y-y_0)^2}{\beta^2}\right]} e^{i[\xi_0 x + v_0 y]}$$

4.3

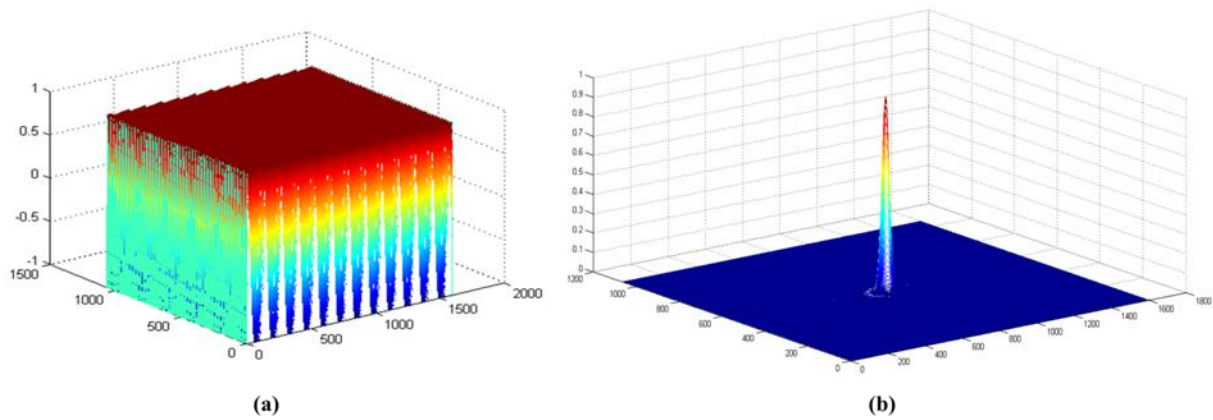


Fig 4.5: a) Waterfall plot of for 2-D Gaussian and complex exponential

i. Vessels Enhancement in retinal images

A 2-D Gabor wavelet filter bank is used to enhance the vessels of image then thresholding is applied to get the binary image containing vascular network. In the first step a green channel of RGB image is obtained and then this obtained image containing this band, is inverted. Inverted green channel and original green channel are shown in fig 4.6

$R_g(i, j)$ represents the inverted green channel image.

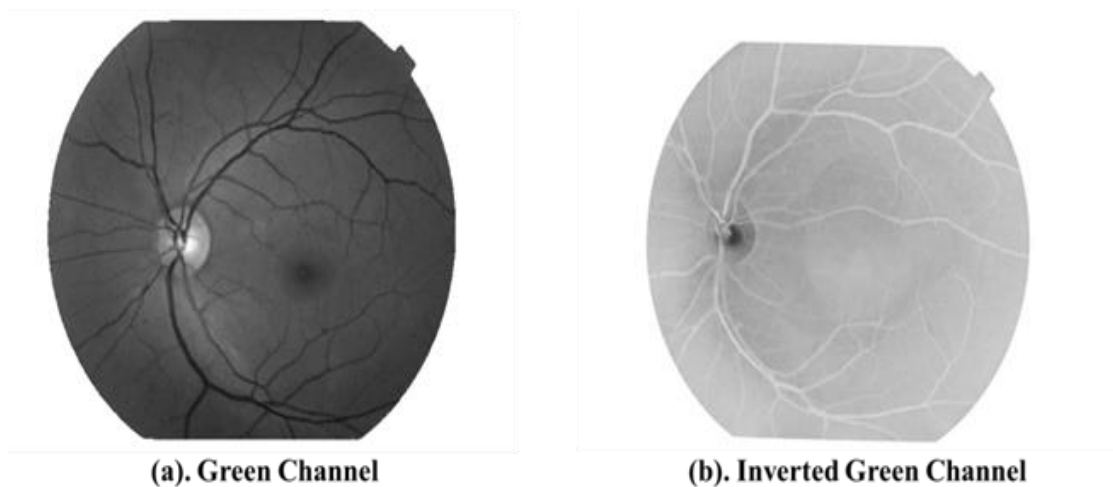


Fig 4.6: (a) Green and inverted green channel images

A 2-Dimensional Gabor Filter is formed which is consist of many orientation and scales. Every filter of this filter bank produce different results. This filter is described in equations [34] as follows:

$$\vartheta_G(\mathbf{x}) = \exp(j\mathbf{k}_o\mathbf{x}) \exp(-\frac{1}{2}|\mathbf{A}\mathbf{x}|^2) \quad 4.4$$

$$\widehat{\vartheta}_G(\mathbf{x}) = (\det B)^{\frac{1}{2}} \exp(\frac{1}{2}(B(\mathbf{k} - \mathbf{k}_o)^2)) \quad 4.5$$

Where $k_o \in R^2$, it defines the frequency of complex part in a vector form, $B = A^{-1}$ and $A = \begin{bmatrix} \epsilon^{-\frac{1}{2}} & 0 \\ 0 & 1 \end{bmatrix}$ with elongation $\epsilon \geq 1$ is a 2 x 2 positive definite diagonal matrix which defines the wavelet anisotropy and elongation of filter in any desired direction. Different orientations of Gabor filter is presented in Fig 4.7

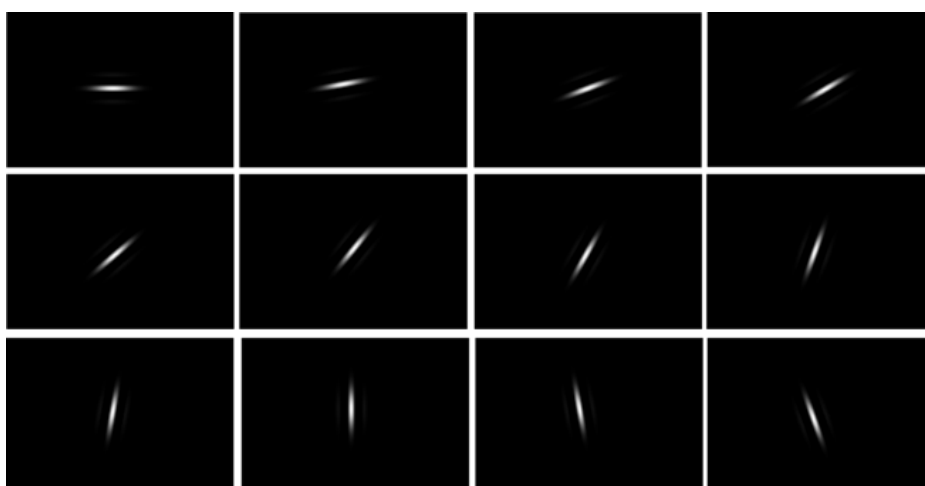


Fig 4.7: different orientations for Gabor Filter

The maximum result is taken from the different results generated when $M_g(\mathbf{b}, a)$ is estimated while taking θ as 0° to 180° with the different of 10. Each pixel is selected and evaluated in this process which considered scale. The equation 4.6 shows the Gabor Wavelet Transform.

$$M_g(\mathbf{b}, a) = \max |T_g(\mathbf{b}, \theta, a)| \quad 4.6$$

Table 4.1 shows the results obtained after applying Gabor Wavelet. Fig 4.8 shows its results at different scales.

Table 4.1: Parameters used for Gabor Wavelet

Equation parameters	Value
Rotation Angle (θ)	10
k_o	[0,3]
Elongation (ϵ)	4
Dilation (a)	3

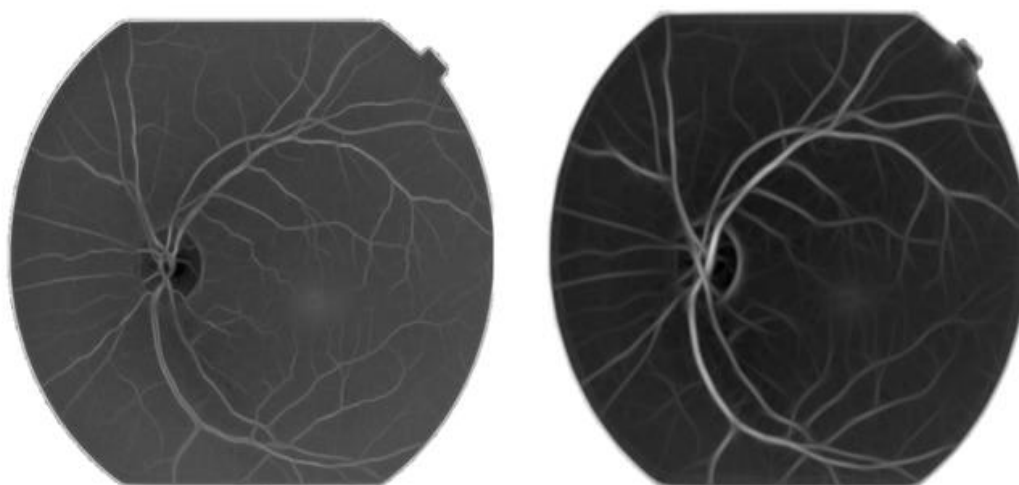


Fig 4.8: Gabor wavelet used for image enhancement using different scales 2, 10

Figs 4.9 to 4.10 thoroughly explains the different scales of Gabor, when we have applied scale=2, the small frequencies are highlighted and small vessels are considered with this scale. As we applied the scale=10, this high scale showed the low frequencies changes which highlights the large vessels, so the large vessels are enhanced as well. Because it gives the high response where frequencies changes ratio is very low.

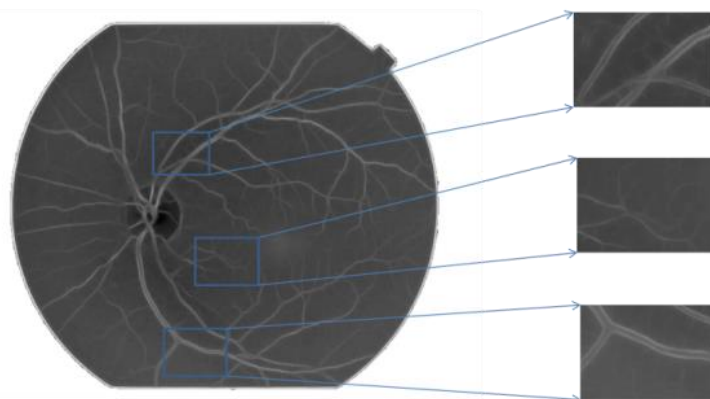


Fig 4.9: enflamed vessels in enhanced image

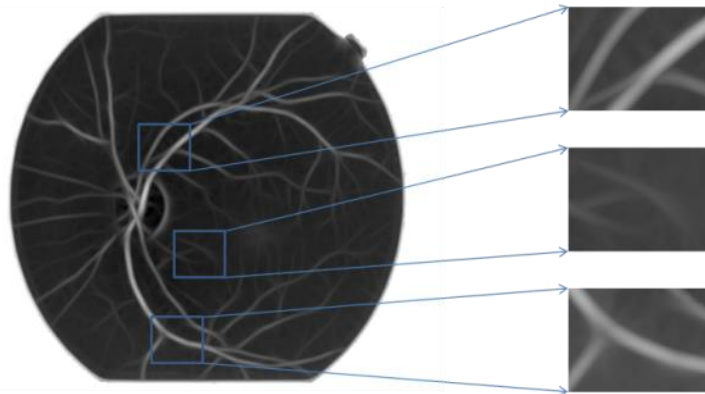


Fig 4.10 showing low frequency response of vessels

ii. Binary image acquisition by Otsu thresholding.

Otsu's thresholding Algorithm is further applied on enhance image to get the binary image. Enhanced image and binary image after thresholding is shown in 4.11 and this vessels response along with original image is seen in fig 4.12. A highly accurate vascular network enhancement is obtained through Gabor Wavelet.

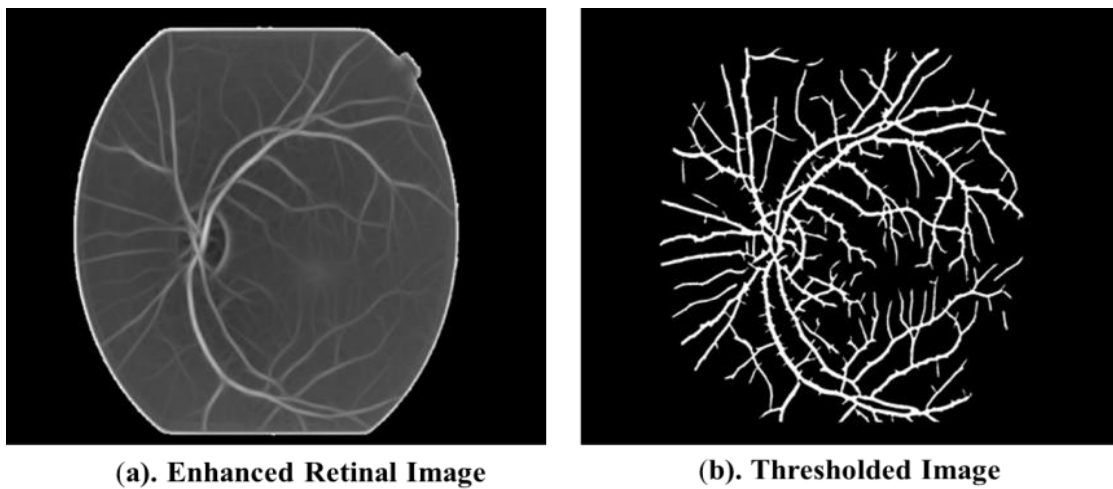


Fig 4.11: a) Enhanced vascular network in image b) Binary image after thresholding

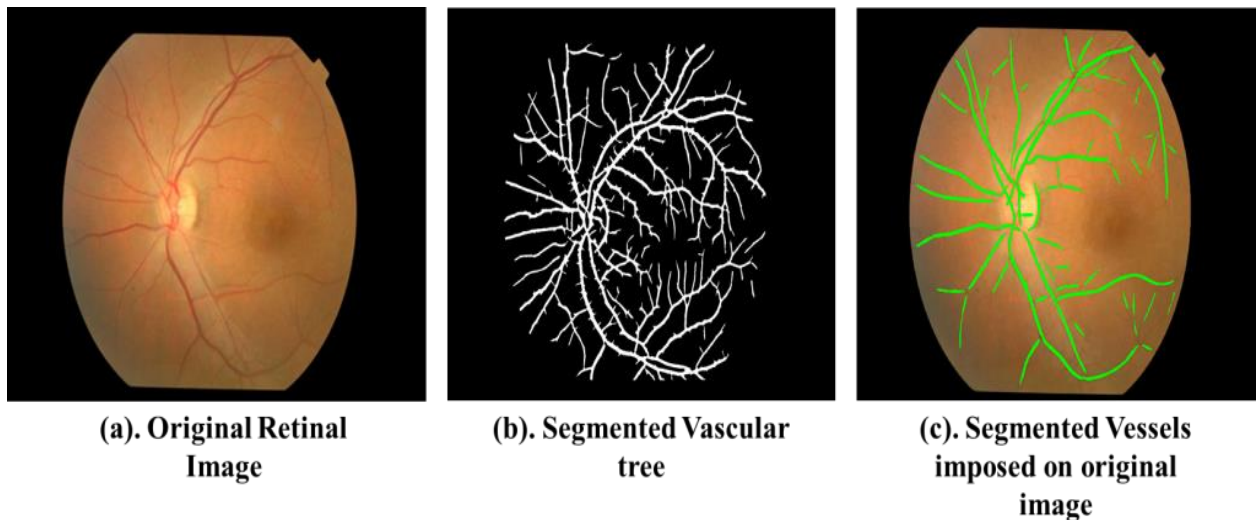


Fig 4.12: a) Retinal color image, (b) vessels in binary image, c) Vessels segmented image imposed on retinal image.

4.3 Optic Disk Detection

After vessel segmentation, OD segmentation is also done before the analysis of the region of interest. This analysis region is used to detect and extract the vessels for classification which are lying inside the region. As the optic disk appears as the brightest area of the retinal image which helps out to pinpoint the OD. This is useful to detect the OD and after it the region of interest. When it is observed the position of optic disk, the area or region of OD is detected and segmented in a binary image. So firstly we have to localize the Optic Disk.

4.3.1 Optic Disk position detection

OD localization is a very sensitive part of this process. As there can be many other regions such as exudates and hemorrhages which are also very bright regions. So it could be possible that OD region is confused with these bright regions. And the system shows that bright regions as OD. So to overcome this confusion it is pre-step to find and save the original location of the OD. It is necessary precaution that if system could not localize the actual position of the optic disk then do it at this step otherwise it could be a costly step to localize it in next segmented steps. This time it is selected the red band of the RGB color space due to the brightness of the optic disk. As the brighter regions are presented fine in this channel. In the fig 4.13 all three bands of color-space are shown.

Localization of the OD is done by implementing the following steps [35].

- A window size of 27x27 for an averaging filter is taken and applied on the image. This step is used to suppress the other areas of the image by smoothing the image.
- After acquiring the whole intensity levels, the region with highest intensity values is selected that is called the OD localization. These Figs 4.13-4.14 shows the results after implementing the averaging filter

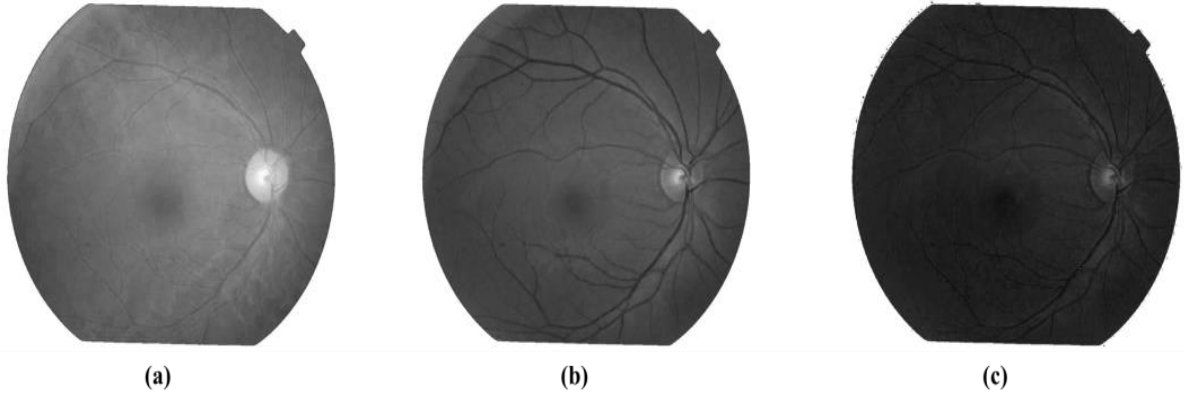


Fig 4.13: a) All three channels of RGB color-space

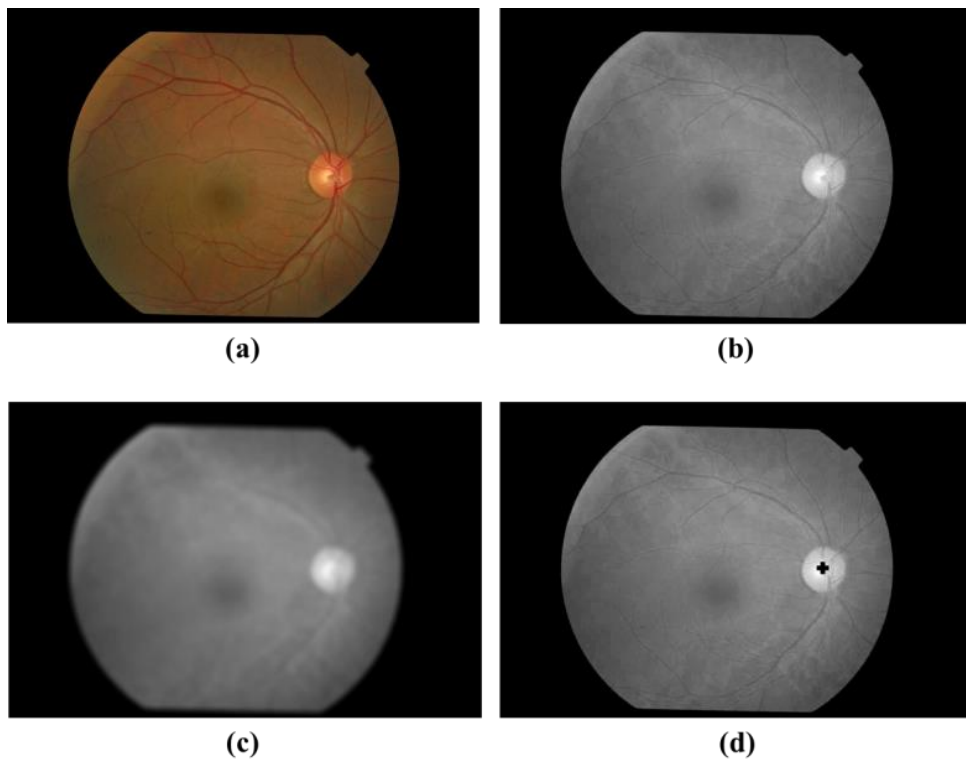


Fig 4.14: (a) Retinal fundus image, (b) Red band of RGB image, (c) filtered image, d) OD position indication

4.4 Identification of Analysis Zone

Region of analysis zone or a region of interest is measured out closely outside the optic disk.

This region is located for the vessels to be classified which are lying within the region. There are many reasons to be defined to select the region of interest around the optic disk as like:

- Vascular network in the retinal image is more rich near the optic disk while weaker the marginal areas of the image. It becomes faint and blur near the marginal areas and away from the OD. A vessel near and far from the optic disk is marked in the Fig 4.15 which shows the vascular trend in the retinal image. Three bands of the RGB image are displayed. The variation in intensity values can be seen in fig 4.15 where these values are changing from close to far from OD.

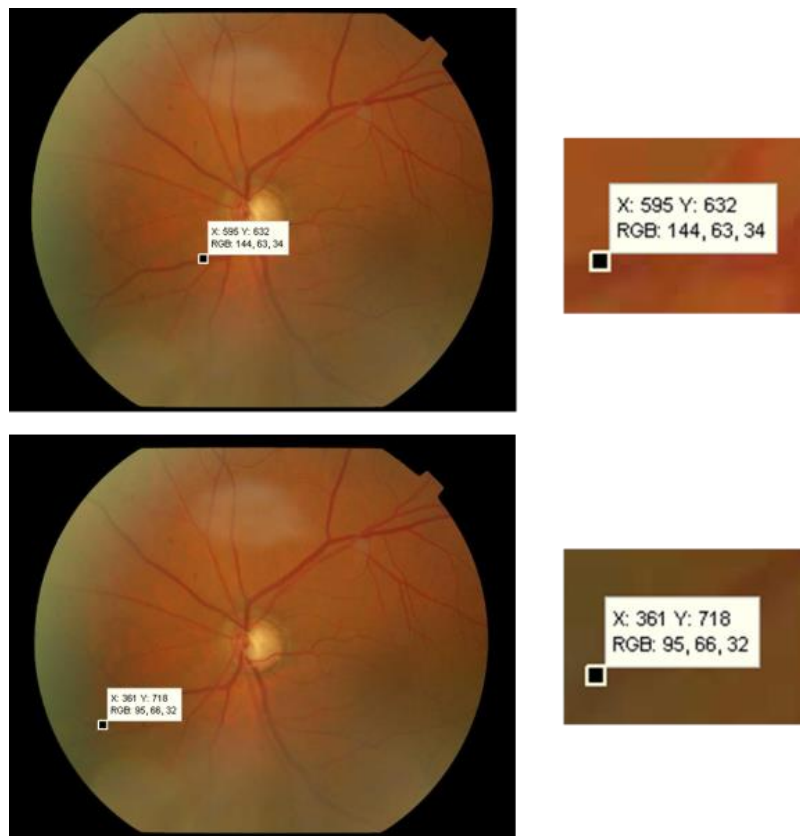


Fig 4.15 RGB image along with the different intensity values of the same vessel

- On the other hand, the size and width of the vessels also varies when it is going from OD to far marginal areas. In Hypertensive Retinopathy, it is observed that the width of vessels is changed also. At the crossing point of two different vessels the width of those vessels is possible to get changed. Width of veins also affected and become less at crossing points due to the arteriovenous crossing. So, it is necessary to have such concentric region where the width of vessels to be constant more likely. Width variation in the vessel can be seen in the fig 4.16.



Fig 4.16 Vascular Structure in retinal image

- Some small vessels which are formed on the retina near the optic disk can also be observed but very difficult to analyze them are shown in the fig 4.17 below. The size and width of these vessels are very small values.

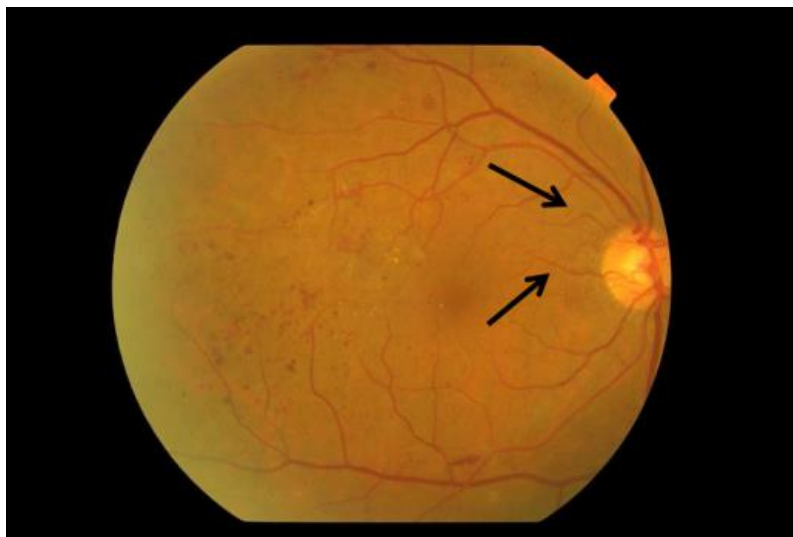


Fig 4.17: a) Retinal image, small vessels formed on retina are pointed

These are some reasons to form a round area about the optic disk to be considered and concentrated. This area is identified for the vessel classification as the vessels containing in this area is to be classified. This step costs very less as there is a partial region to be computed which carries very less computation as well. This region is taken around the optic disk about to half meter in diameter in the form of circular margin lines and named as region of interest

(ROI). In the fig 4.18 the center is marked of the optic disk as segmented OD and other one is the OD with region of interest mentioned.

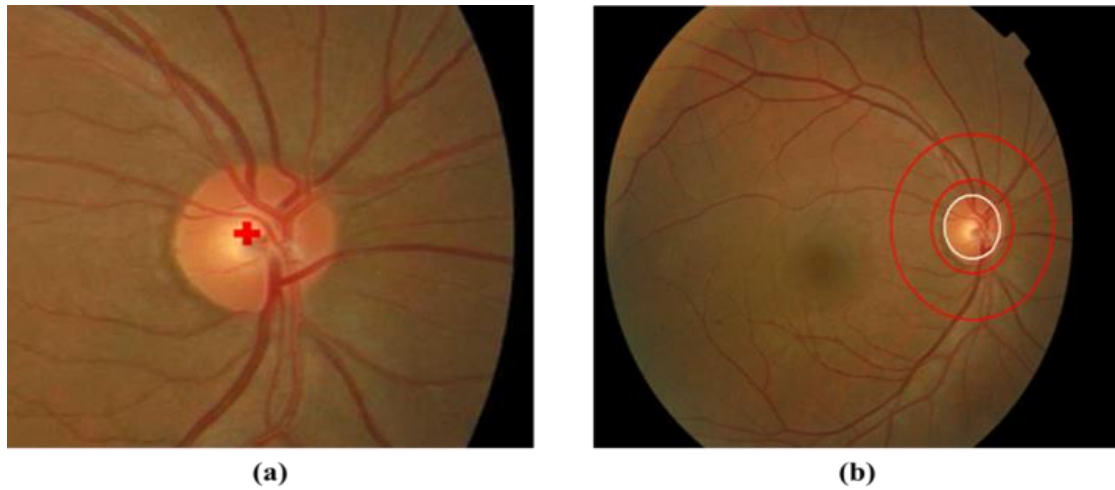


Fig 4.18: (a) OD position and center detection, b) OD region of interest marked

4.5 Vessels classification into arteries and veins

Blood vessels classification in the research is carried out as pixel-wise along with region-wise. This combination of two process is responsible for the accurate classification. Three type of features are extracted including color, texture and shape features.

4.5.1 Feature Extraction

This step of the research is related to the feature extraction from the image which map the properties of image objects to form a feature vector which assures the help in separation or clarification of those objects of the image. Feature extraction is the extraction of those features from vessels which are responsible to classify the vessels into arteries and veins. These are two types of features. Profile based features and center-line pixels. Artery feature space shows the specific features belongs to artery and same on the other hand as well for veins. Color features are extracted by exploring the different color spaces like CMYK, RGB, NTSC, HSV, YCbCr, CIE L*a*b and OPP color spaces. These color features are found from the different parts of the vessel. These points includes the centerline pixels and the pixels lies at the boundary of vessel. These points can be seen in the fig 4.19-a which includes the pixels of two areas. Fig 4.19-b shows the profile based features.

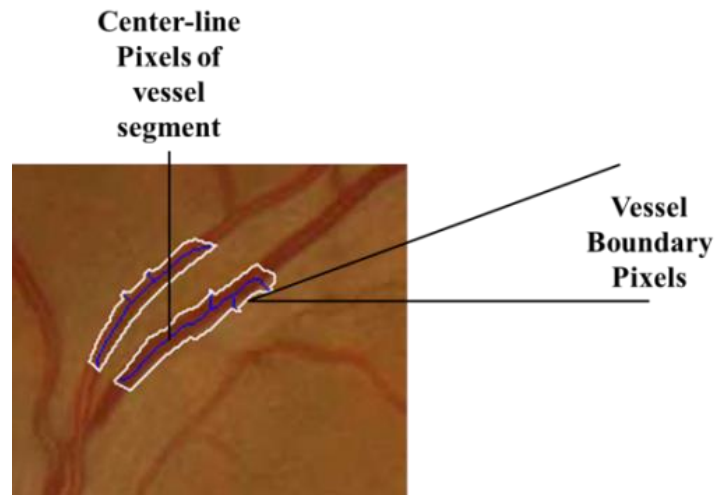


Fig 4.19-a: retinal image with centerline pixels of a vessel segment

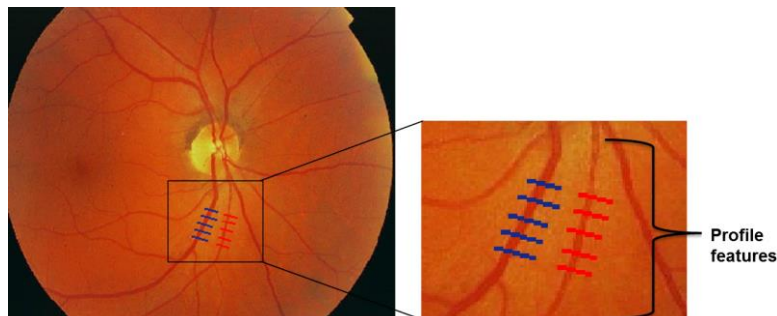


Fig 4.19-b: retinal image with horizontal profile based features of a vessel segment

Retinal blood vessels are classified into arteries and veins using many filters. Classification is carried out on the basis of four type of features. These all features are selected on the basis of human perception about the vessels appearance and visualization. Some of them are described by the ophthalmologists on the basis of clinical findings which are widely used by ophthalmologists in manual classification. Here is stated a description of all type of features which are extracted.

- First of all the most important and widely used in different researches are color features. As the quantity of oxygen is larger in arteries which make them brighter in color-space is the key point of differentiation of two types of vessels. The feature set comprises of the brightness of centerline pixels, boundary pixels, and pixels at the starting and ending points of the vessels.
- The orientation and arrangements of the pixels are combine in texture feature set, this also helps in separation f vessels by calculating the statistical parameters.
- The size and shape features which are a strong descriptor as veins are usually wider

than arteries. Thus, it results in compression of arteries in the presence of AVR.

Features extracted are illustrated below.

1. Mean value and third moment of (f1, f2) centre-line pixels of vessel segment in red channel of RGB image.
2. Entropy and relative smoothness (f3, f4) of vessels centre-line pixels in Green channel of RGB color-space
3. Mean value and uniformity (f5, f6) of vessel center-line pixels in M-channel of CMYK color-space
4. Variance (f7, f8, f9) of center-line vessel pixels in all three channels of L*a*b color-space
5. Mean value (f10, f11) of vessel center-line pixels in Luminance and Chrominance components of YCbCr color-space
6. Minimum value (f12, f13) of pixels in profiles of vessel segments in green and blue channel of RGB color space

Color features are illustrated visually in Fig below, which are plotted in the form of intensity profiles. These plots describes the intensity profiles in different spaces. These are shown the intensity values of arteries and veins in RGB, CMYK, HSV and LAB color spaces respectively from fig 4.10 to 4.24.

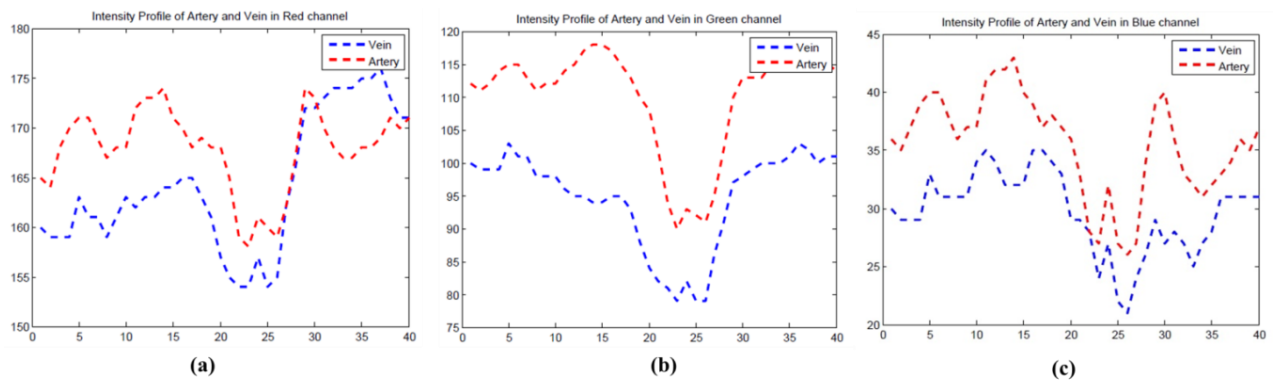


Fig 4.20: a). Intensity profiles in all three channels of RGB color-space

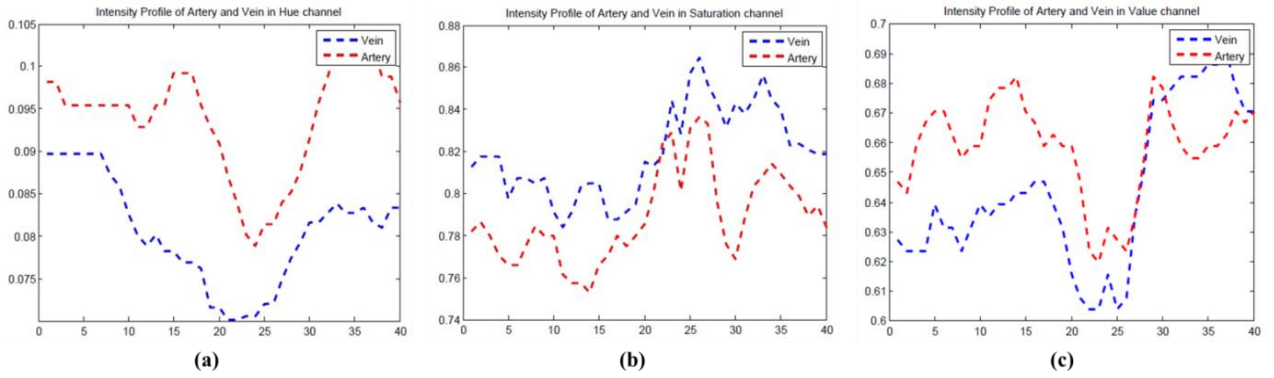


Fig 4.21: a). Intensity profiles in all three channels of HSV color-space

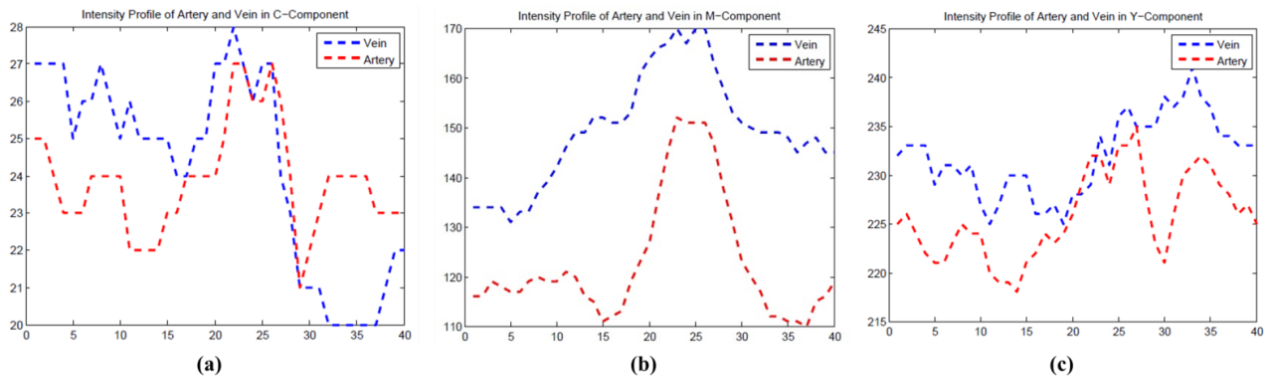


Fig 4.22: a). In C- channel the intensity profile of vessels b). Intensity Profile in M channel in CMYK color-space, c). Intensity Profile of both type of vessels in Y channel

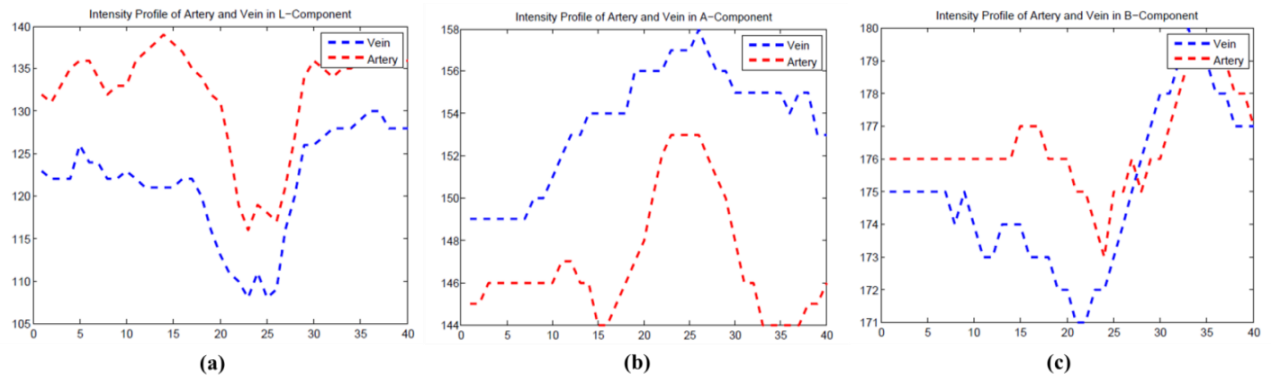


Fig 4.24: Intensity profiles in all three channels of La*b* color-space

4.5.2 Feature Selection

These extracted features are used for the classification of vessels. For the classification purpose it is necessary to exclude those features which are no more useful for classification and include all those features which contribute at higher level in classification. So the features which lower

participation in classification are removed and does not includes in the process. More of the features addition leads to more dimension which results in the poor performance of the classifier. It is observed that the features increment is useful for the better performance but at some level the performance achieves the peak and after that the increment in feature set the performance starts to get lower at same amount of samples [43]. This is the reason that feature selection step is included in this whole procedure.

Features are selected by two type of techniques mostly, named as wrapper method technique and filter method. Wrapper method technique used the performance of classifier to select the features [44]. And the other techniques simply selects the features on their own ability to classify the features. These feature selection is purely depend upon the features ability. This research is also done by using one of the later described technique; filter method. This method is called Wilcoxon rank test. After applying this test on all features only the top five features are selected with higher values.

Table 4.2 shows the features with their values obtained and which are selected for the classification.

Table 4.2: Wilcoxon test results of features with p-value.

Features	Score	P-Value
f5	5.4264	< 10⁻⁶
f3	5.3824	< 10⁻⁶
f9	5.1628	< 10⁻⁶
f10	4.8552	< 10⁻⁶
f6	4.8332	< 10⁻⁶
f7	4.3499	0.00001
f8	3.9984	0.00006
f11	3.7128	0.0002
f12	3.5055	0.0004
f1	2.6363	0.0084
f2	2.5229	0.0116
f13	1.0216	0.307
f4	0.681	0.4958

Boxplots are used to visually describe these features for both participants of the vessels. This representation shows the graphical view of both classes of maximum and minimum, and median values. Boxplot are given for the top five features in the fig 4.28. while fig 4.29 to 4.36 shows other features boxplots.

These features and the Median values are represented in box plots to see differentiation visually. Box plot represents the features visually like max value, min value, median value and upper quartile of different color spaces. Fig 4.28 shows the top valued features in box plot representations.

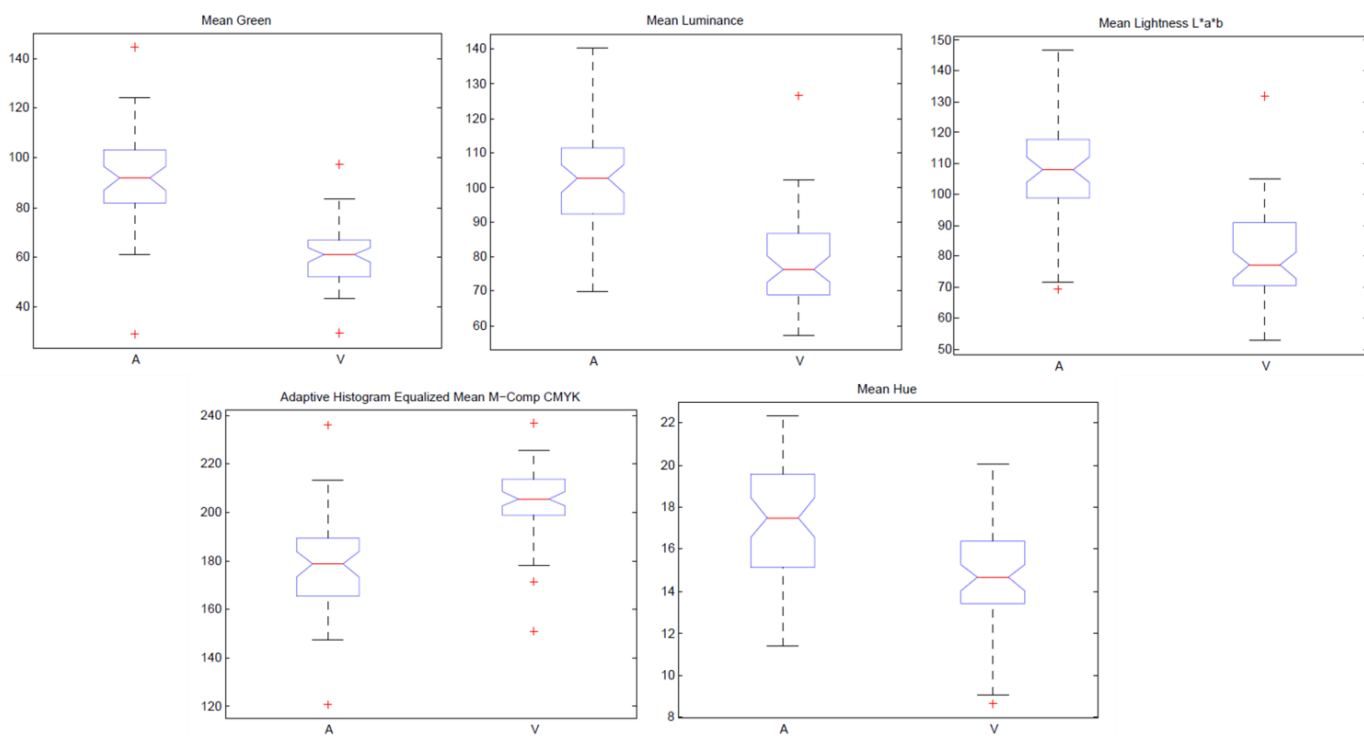


Fig 4.28: Top five selected features in Box Plot representation

4.6 Width measurement and AVR calculation

After the feature selection these vessels are classified into arteries and veins then the width of both type of vessels is calculated. 2-D Euclidean distance transform methodology is used to estimate the width of the vessels [45]. This transformation is done by converting the binary image into gray-level image where intensity level values are not shown on pixels, instead it is shown the distance values of that pixel to the nearest non-zero pixel. Many steps are involved in this transformation process. These steps are explained below and demonstrated in Fig 4.37.

1. Segmented binary image containing the vessels is complemented

2. These image is further processed with 2-D Euclidean distance transformation.
3. A morphological operation thinning is applied to get one pixel wide vessel tree.
4. This image with centerline pixels only is further multiplied with the 2-D Euclidean distance transformed image to get the values of center pixels.
5. These obtained values are doubled to obtain real value of width of the pixels.

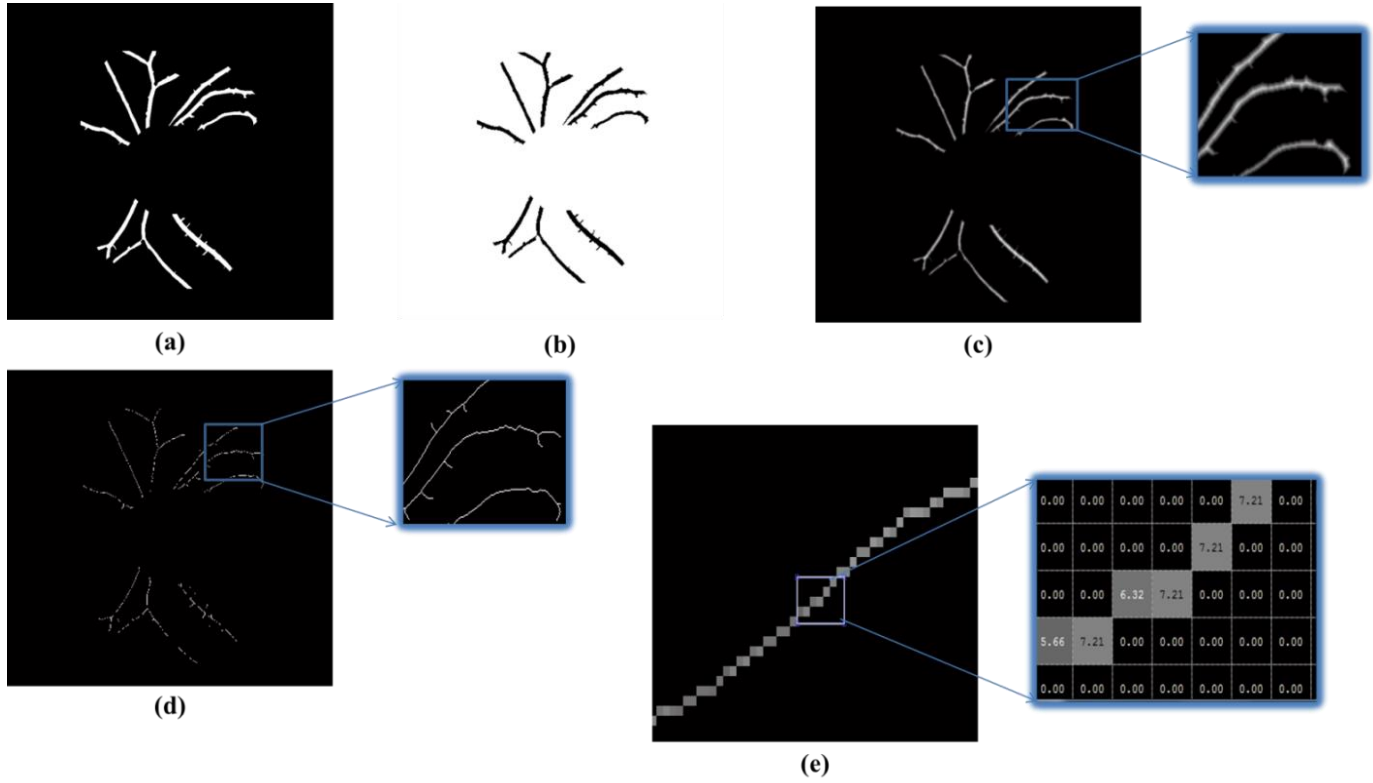


Fig 4.37: Vessel Width Estimation, a). Retinal binary segmented image, b). Complement of image a), c). Distance values of vessel pixels, d). One pixel wide vessels binary image, e). Multiplied image of (c) and (d)

4.6.1 Calculation of AVR

Two parameters are used for the calculation of AVR which are Central Retinal Venous Equivalent (CRVE) and Central Retinal Arterial Equivalent (CRAE). Parr-Hubbar proposed these two measures [46]. Arteriole and Venule are vectors which contains the mean of width of both type of vessels.

These parameters are measured by using equations 4.8 and 4.9.

$$CRAE = \sqrt{(0.87W_a^2 + 1.01W_b^2 - 10.73 - 0.22W_aW_b)} \quad 4.8$$

Where W_a is the value of width parameter before the value of median and W_b is the value of the median.

$$CRVE = \sqrt{(0.72W_a^2 + 0.91W_b^2 + 450.02)} \quad 4.9$$

Here width values represents the same values for veins.

Equation 4.10 shows the formula for AVR calculation.

$$AVR = \frac{CRAE}{CRVE} \quad 4.10$$

4.7 Detection and classification of Papilledema

Extra vascular changes are also become the cause of Hypertensive Retinopathy. These extra vascular changes are consist of hard and soft exudates, Microaneurysms and optic disk swelling. Along with the exudates, papilledema is also an extravascular change which causes hypertensive retinopathy is actually swelling of Optic Disk. It appears as the severe stage of Hypertensive Retinopathy. This swelling of optic disk is due to reduced flow of nerves in optic nerve head [47]. The changes in the exoplasmic flow (intracellular or extracellular) causes in swelling of optic nerve head which is called papilledema [48]. It is urgent for the patients suffering with OD swelling to cure as soon as possible. This also can be a cause for vision loss and as well as formation of other diseases [49]. Retinal fundus images are also have advantage to detect the papilledema.

For the grading of papilledema, Frisen has introduced a grading scheme of 6 stages which are involved to have papilledema [50]. This grading scheme starts from normal (0) to severe (5). These stages of papilledema are categorized on the basis of some visual feature set. Frisen scale is observed as the best grading scheme but Scott et al. has modified the previous grading scheme by adding and identifying some more basic features and modifying the Frisen's features [51]. This grading scheme is shown in the table below.

TABLE 1. The Modified Frise'n Scale

Grade	Clinical Signs
Grade 0	No Signs
Grade 1	A grayish color C-type ring is formed ; disappearing to retinal information

	Normal temporal disc margin but obscured nasal disc margin
Grade 2	Circular shaped ring Temporal disc margin misplaced as well as nasal disk. No major vessel vagueness
Grade 3	Ambiguos , but not obscured in the center Elevation, proximately all borders Ring, irregular outer fringe with finger-like Extensions
Grade 4	Total obscuration of a segment of a major artery or vein at its central origin Ring, complete
Grade 5	Obscuration of all vessels both on the disc and leaving the disc

Fig 4.39 is shown below which describes the flow chart of detection of papilledema.

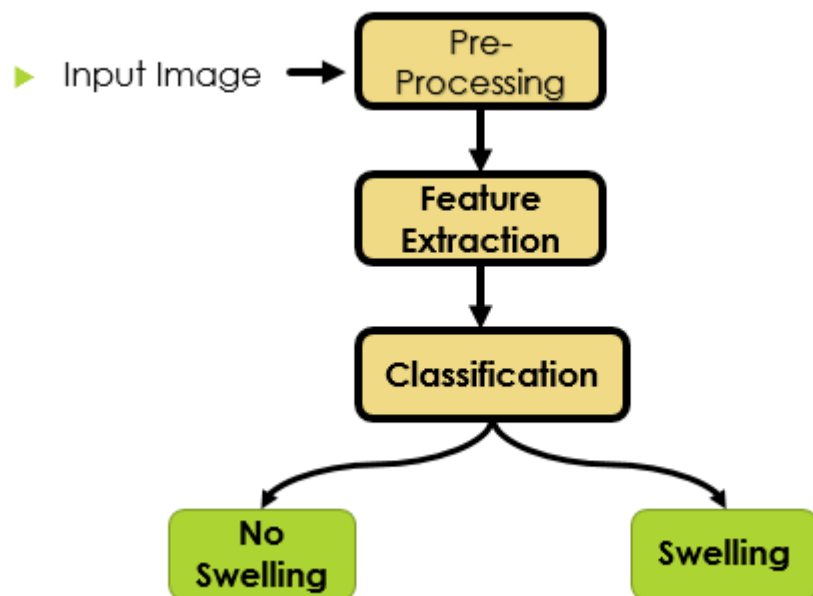


Fig 4.39: Flow chart for papilledema detection

4.7.1 Pre-Processing and Vessel segmentation

- ***Pre-processing***

The retinal image is taken for the pre-processing for the sake of noise removal and separation of background and foreground. Median filter is applied to blur the sharp noisy pixels of the image [52]. This filter also helps out to remove the artificial factors like local luminosity and contrast inconsistency. These factors add up in the time of image acquisition and make information complex. Green channel which contains unsaturated information is used for the filtering.

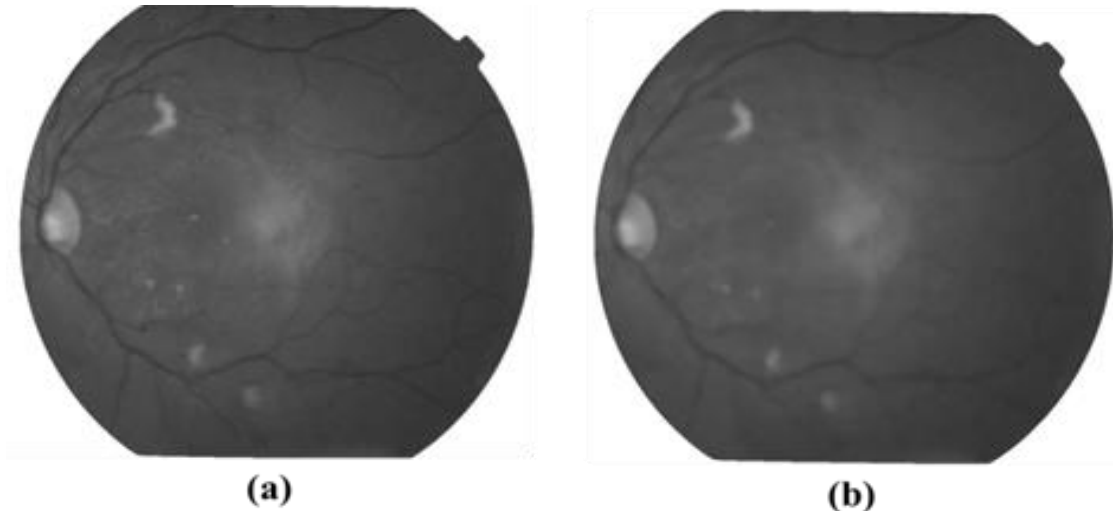


Fig 4.40: (a) Green band image of retina, (b) Resulting image after filtration

This filtered image is further used in vessel segmentation to get the vasculature features which are used in classification. Vessel segmentation is done using a technique already used for segmentation for vessel classification. 2-Dimension Gabor Wavelet filter bank is responsible for the vessel segmentation and enhancement. This technique is used because there is a lot of pattern and texture information in the image which returns a high response when it matches with the relevant filter from the 2-D Gabor wavelet [53]. A threshold is applied to the enhanced image to get the binary segmented image.

Image enhancement and segmentation is shown below in Fig 4.41

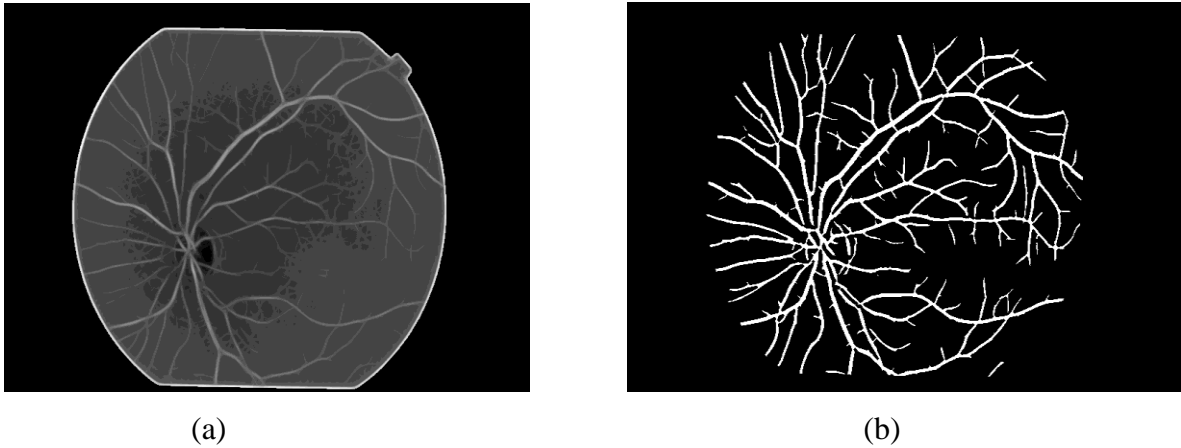


Fig 4.41 a) Enhanced image b) Segmented Image

Next step of pre-processing is the detection of OD which is done as like we did it in the vessel categorization.

- ***Elimination of Blood Vessels***

Before going to classify the images into classes, the vessels are removed within the area of Optic disc. The disc margin is very important to calculate due to the features related to disk margin obscuration. This vessel removal process is done using technique which is used by Criminisy et al. [58]. These vessels contribute only 5% to the disk margin that's why we exclude them.

- ***Optic Disk margin selection***

Optic disk boundary is very important for the grading of papilledema. Because the swelling of optic disk is occurred when the boundary pixels are misplaced. To get the parapapillary texture features, OD margin is selected. This is done using contrast and intensity variation of the pixels. From the center of the optic disk the pixel whose intensity gradient is changed is selected. This margin is selected at radial distance from the optic disk center. Fig 4.42 shows the abnormality in disk margin obscuration.

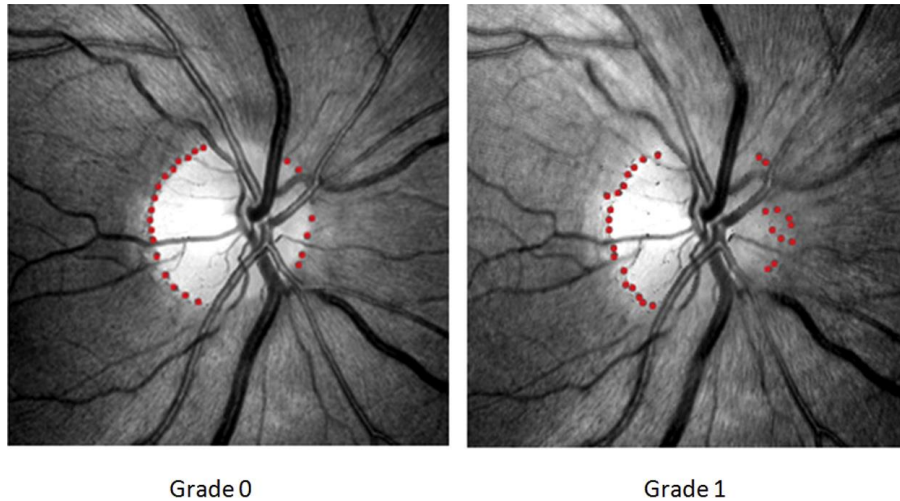


Fig 4.42 Optic disk margin is selected from the center of OD for different grade of papilledema

4.7.2 Feature Extraction

After completing the first step, the next step for this methodology is feature extraction. As we know it is very severe stage of hypertensive retinopathy and very difficult to grade by an automated system. Ophthalmologists manually grade this by using different type of features. Total four type of features are considered per ophthalmologists advice which are 1) vasculature network changing features, 2) optic disc boundary changes, 3) parapapillary colored texture features at surrounding of optic nerve, 4) RNFL changes (Retinal Fiber Nerve Layer). These features are completely considered by the ophthalmologists which used them for manual grading. Table 4.3 shows the features which are extracted type wise.

Total 12 features used for the processing of algorithm are shown below.

Parapapillary Texture features

- 1) Contrast values in overall region
- 2) Correlation of pixels in overall region
- 3) Energy of pixels in overall region
- 4) Shade difference of pixels of inside and outside of disk
- 5) Entropy of the overall region

Blood Vessel Features

- 1 Mean of area of regions in vascular network
- 2 Vessel discontinuity index
- 3 Largest vessel are in vascular network
- 4 Skewness of area distribution on the regions in the vascular network
- 5 VDI within disc area

- 6 Standard deviation of the regions in the vascular network
- 7 Smallest vessel area in retinal vascular network

4.8 Classification by Support Vector Machine

All extracted features of the images in different color spaces are given to SVM classifier which are classified into two types. These features are given to the classifier in training set with their label assigned by ophthalmologists. Then it separates the features. A normal vector μ and another parameter offset ρ is used to define hyperplane which separates the features given in equation below [52].

$$h.p = \{x|\langle u, x \rangle + p\} \quad 4.15$$

$$\text{Where } \langle u, x \rangle + p = 0$$

It separates feature image in test set into two classes, arteries and veins. This classification is done by SVM classifier.

In papilledema it classifies the images into swelling or not swelling.

CHAPTER 5: EXPERIMENTAL RESULTS

In this chapter, analysis of vessel classification and OD swelling detection is done and their performance is evaluated. Veins are annotated as blue and arteries as red by doctors. This annotation is done using MATLAB based tool. The area of OD is also annotated. These annotated retinal images are used to compare the results of proposed method. Three datasets are used for this research. Each of datasets are described below in detail.

5.1 Datasets

- *VICAVR*

This dataset is consists of publically available retinal images which are available for the AVR computation. These are cropped retinal images centered at OD. This database has total 58 images. Resolution of these images are 768x584. These database images are labeled by three ophthalmologists. Total 418 segments of vessels are included in this dataset for validation purpose.

- *INSPIRE-AVR Database*

This dataset includes images with resolution of 2392x2048. Total 40 images are included in this dataset. This dataset used reference standard for AVR. This standard is related to the average evaluation by two experts by using a program IVAN which is developed in University of Wisconsin, WI, USA. These 40 images contained total 301 vessels segments which are considerable. Fig 5.1 contains the imaged from INSPIRE-AVR daabase.



Fig 5.1: INSPIRE-AVR database images

- *Local Database*

This automated proposed technique was also analyzed for vessel classification and detection of papilledema, a local database is also used for this purpose. This database consist of 30 images with resolution 1504x1000. These images of local database were provided by the AFIO (Armed Forces Institute of Ophthalmology), Pakistan. 9 of 30 images which are involving in the existence of papilledema. These images are provided with background mask images.

Fig 5.2 shows images from local database

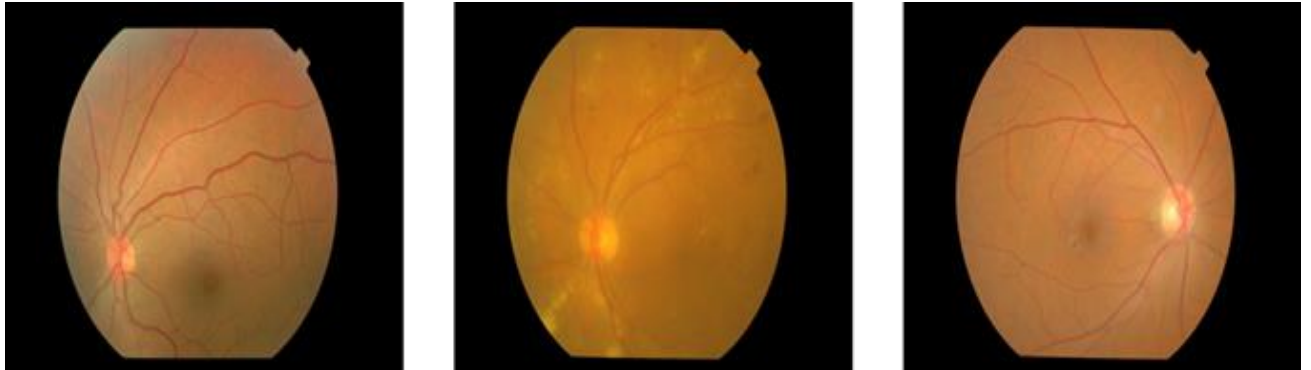


Fig 5.2: Images from AFIO database

These all three databases are annotated by the ophthalmologists. Diseased or affected images are mentioned by the specialists. Table 5.1 shows the description of datasets according to the annotation.

Table 5.1: Datasets with annotated data by the ophthalmologists.

Database	AFIO	VICAVR	INSPIRE-AVR
Total Images	32	58	40
Normal Images	24	45	33
Diseased Images	8	13	7

5.2 Results

5.2.1 Vessel Classification Results

First vessel classification is done and its results are also explained first. These results of vessel classification are also compared with old results of other proposed methods for vessel classification. Some main evaluated factors are described below.

1. Evaluation Parameters

This proposed system is evaluated by some parameters which are accuracy, specificity, sensitivity and PPV as positive predicted value. True positive rate of results are named as sensitivity and true negative rate is called specificity. These factors of accuracy is estimated for both type of vessels i.e. arteries and veins. These listed below equations are used for the calculation of these parameters. Equation 5.1 to 5.4 are these equations. And fig 5.3 shows the images with results.

$$Sensitivity = \frac{T_P}{(T_P+F_N)} \quad 5.1$$

$$Specificity = \frac{T_N}{(T_N+F_P)} \quad 5.2$$

$$PPV = \frac{T_P}{(T_P+F_P)} \quad 5.3$$

$$Accuracy = \frac{(T_P+T_N)}{(T_P+T_N+F_P+F_N)} \quad 5.4$$

Vessel classification by this system is shown below in fig 5.3 where arteries are shown as blue and veins as red. Table 5.2 shows the results, and performance values for vessel classification by comparing with other results for VICAVR dataset are in table 5.3. Table 5.4 shows its comparison with other techniques.

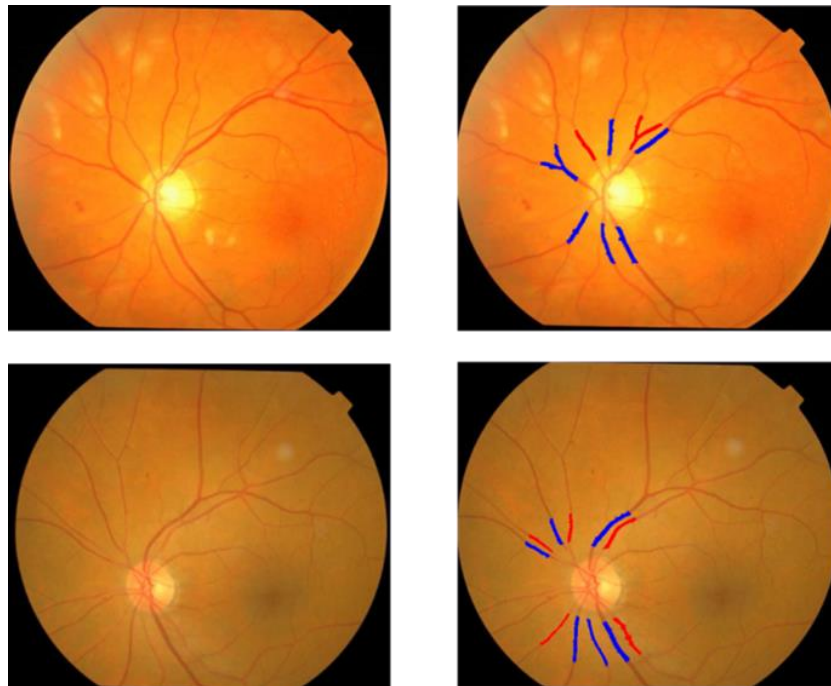


Fig 5.3: Original image with classified image representing vessels as arteries as red and vein as blue

Table 5.2: Performance measures with values

Performance Measure	Arteries	Veins
Accuracy	0.8727	0.8636
Negative Likelihood Ratio	0.1800	0.1112
Negative Predictive Value	0.8474	0.9000
Positive Predictive Value	0.9019	0.8333
Positive Likelihood Ratio	9.2000	4.9972
Specificity	0.9200	0.8181
Sensitivity	0.8263	0.9090

Table 5.3: Comparison with the previous systems Using VICAVR dataset

Authors	Accuracy	Dataset	Classifier
Malek et al. [40]	0.8633	VICAVR	Neural Classifier
Vzquez et al.	86.34%	VICAVR	K-means Clustering
Proposed Method	96.31	VIC-AVR	SVM

Table 5.4: Comparison with previous systems

Authors Name	Accuracy	Database	Specificity	Sensitivity
D. Relan et al [40]	0.8633	Local dataset	0.9284	
G. Mirsharif et al. [38]	0.8600	DRIVE	---	---
Saez et al. [39]	---	Local Dataset	0.892	0.782
Vzquez et al.	86.34	VICAVR	---	---
Murmatsu et al. [2]	0.75	DRIVE	---	---
Proposed Method	96.31	VIC-AVR	0.9200	0.8263
	95.86	INSPIRE-AVR	0.954	0.9542

	95.54	Local Dataset	0.9491	0.8183
--	--------------	----------------------	---------------	---------------

5.3 Papilledema Detection

Papilledema is detected and classified and these evaluation done by comparing its results with the images given in ground truth by the ophthalmologists. They manually annotated the images according to the MFS grading and then this ground truth images are compared with the images which are generated by our system. 82% accuracy was achieved by the system.

Table 5.5 gives dataset specifications.

1. Evaluation Measures

- If the extracted features for papilledema in images correlates with the ground truth images, then it is related to True Positive (T_p).
- If a feature presence is detected in the image but not told in real images then these are related to False Positive (F_p).
- If obscuration of any type is not detected in the image and its present in manually labeled image then that image will denote as False Negative (F_N).

Table 5.5: Dataset Specifications

Total Images	Normal	Images containing OD Swelling
32	22	10

Our algorithm was tested for many comparisons and produce different results after comparing with the ground truth. 82.21% of sensitivity measure is achieved. Table 5.6 shows the confusion matrix for the actual value and predicted outcomes of the dataset.

Table 5.6: Papilledema Detection Results Confusion Matrix

	Prediction Outcome			Total
		0	1	
Actual Value	0	21	1	22
	1	3	7	10
	Total	24	8	

Table 5.7 shows performance evaluation of this proposed algorithm for the detection of optic disk swelling.

Table 5.7: Performance Evaluation of Detection of Papilledema

Parameters	SVM
Sensitivity	95.45 %
Specificity	70 %
Accuracy	82.21%

CHAPTER 6: CONCLUSION AND FUTURE WORK

6.1 Conclusions

Analysis of fundus retinal images is very helpful in detection and diagnosing of different eye diseases at initial stages. These automated systems are also helpful for the eye ophthalmologists as well as diagnosing of disease. Microvascular structure is completely examined by the retinal images analysis and it is very useful as well. Hypertension affects the vessels; and retinal vessels are also affected by this disease. So, the retinal imaging is very important to detect this diseases.

What is the damage done by hypertension is called “Hypertensive Retinopathy”. Many of the technologists and experts from engineering field have been trying to develop an automated system to detect the disease accurately. This research also done for an automated system which helps out for the detection of HR. Health experts mention the clinical findings, which are the base of our automated system. This automated system consist of an algorithm which analyze the image for clinical signs, then categorize the image into different stages of HR. Both type of changes (vascular and non-vascular) are mainly cause for HR. this system detects both of changes and using different digital images techniques. The target algorithm has been completed by coding these techniques. This method comprise of four main parts of system research; noise removal and pre-processing of fundus image, vessels detection and segmentation, classification of vessels and finally measurement of AVR and grading of papilledema. Thus, the research completely emphasis on the correct classification of vessels and the detection of papilledema. The system got 87.27% accuracy and 82.21% sensitivity for detection of papilledema.

6.2 Contributions

This thesis mainly contributes in

- Complete automatic examination of disease Hypertensive retinopathy.
- Two main effects of disease are thoroughly observed i.e. changes in vascular network and optic disk swelling.
- Different features of many color-spaces are accumulate to get results
- These results are also compared with the older techniques.
- 88.27% accuracy for the system is obtained with specificity and sensitivity of 92% and 88.63%, respectively, in classification of vessels, while gives sensitivity of 82.21% for Optic Disk swelling detection.

6.3 Future work recommendations

6.3.1 Detection of abnormal occlusion of vessels.

This research can be used to detect the more vascular signs for detection and measurement of arterio-venous ratio and the classification of vessels. These signs like change in vascular network and formation of other spots in retina and unusual arterio-venous crossing are more important which are covered in this research and in future more research can be carried out.

6.3.2 Tele screening System for HR

This research can also help the ophthalmologists to have a software with GUI made by this algorithm. This software can be made available at low cost. Customization of this software can also be available for doctors it means that they can change preferences accordingly.

References

1. Marco Foracchia, Enrico Grisan, Alfredo Ruggeri, “Luminosity and contrast normalization in retinal images”, *Medical Image Analysis* 9 (2005) 179–190.
2. Chisako Muramatsu, Yuji Hatanaka, Tatsuhiko Iwase, Takeshi Hara, Hiroshi Fujita, “Automated selection of major arteries and veins for measurement of arteriolar-to-venular diameter ratio on retinal fundus images”, *Computerized Medical Imaging and Graphics* 35 (2011) 472– 480.
3. Lee, Y.; Lin, R. S.; Sung, F. C.; Yang, C.; Chien, K.; Chen, W.; Su, T.; Hsu, H.; Huang, Y. (2000). "Chin-Shan Community Cardiovascular Cohort in Taiwan-baseline data and five-year follow-up morbidity and mortality", *Journal of clinical epidemiology* 53 (8): 838–846.
4. Patrick J. Saine and Marshall E, “Ophthalmic Photography: Retinal Photography, Angiography, and Electronic Imaging”, 2nd Edition, Tyler Butterworth-Heinemann Medical; ISBN: 0750673729.
5. Conti, Fiorenzo, “Fisiología Médica”, (1st edition), Mc-Graw Hill.
6. J.J. Staal, M.D. Abramoff, M. Niemeijer, M.A. Viergever, B. van Ginneken, "Ridge based vessel segmentation in color images of the retina", *IEEE Transactions on Medical Imaging*, 2004, vol. 23, pp. 501-509.
7. Karenchantek, “Hypertensive Retinopathy vs Diabetic Retinopathy”, karenchantek’s blog, October 4, 2013.
8. Ruggeri A1, Grisan E, De Luca M, “An automatic system for the estimation of generalized arteriolar narrowing in retinal images”, *Proceedings of the 29th Annual International Conference of the IEEE EMBS, Cité Internationale, Lyon, France, August 23-26, 2007*.
9. Jack J. Kanski, “Clinical Ophthalmology: A systematic approach” (6th edition).
10. Louise O’Toole, “Hypertensive Retinopathy: Referral Refinement Part 9,” FEBO C-16903 O/D.
11. Joseph B. Walsh, Richard B. Rosen and Daniel M. Berinstein, “Systemic Hypertension and the Eye,” Chapter 13.
12. Scheie HG, Ashley BJ, Yanoff M, “Medical ophthalmology: Hypertension and arteriosclerosis,” *Ophthalmologic Manifestations of Systemic Diseases*, p 17. Elgin, IL: Medicolor Illustration and Editorial Service, 1966.
13. Local dataset taken from AFIO, Pakistan.

14. Arterial tortuosity syndrome, genetics home reference
'<http://ghr.nlm.nih.gov/condition/arterial-tortuosity-syndrome>'
15. Hamid Reza Pourreza et al., "Simple and Efficient Method to Measure Vessel Tortuosity", 3rd International Conference on Computer and Knowledge Engineering (ICCKE 2013).
16. The free medical dictionary, <http://medical-dictionary.thefreedictionary.com/Retinal+hemorrhage>.
17. The COMS Grading Scheme: Graded Features Retinal Hemorrhage, <http://webeye.ophth.uiowa.edu/>.
18. Ophtho Book, <http://www.opthobook.com/>.
19. N. M Keith, H. P. Wegener, and N. W. Barker, "Some different types of essential hypertension: their course and prognosis", *American Journal of Medicine Science* 197 (1939), 336-354.
20. H. G. Scheie, "Evaluation of ophthalmoscopic changes of hypertension and arterial sclerosis", *Archives of Ophthalmology* 49 (1953), no. 2, 117.
21. Wong TY, Mitchell P, "Hypertensive retinopathy", *N Engl J Med* 2004.
22. A Grosso, F Veglio, M Porta, F M Grignolo, T Y Wong, "Hypertensive retinopathy revisited: some answers, more questions," *Br J Ophthalmol* 2005;89:1646–1654.
23. Narasimhan et al, "Hypertensive retinopathy diagnosis from fundus images by estimation of AVR," *Hypertensive retinopathy diagnosis from fundus images by estimation of AVR*.
24. Alfredo Ruggeri, Enrico Grisan, Massimo De Luca, "An automatic system for the estimation of generalized arteriolar narrowing in retinal images", 29th Annual International Conference of the IEEE EMBS Cité Internationale, Lyon, France, August 23-26, 2007.
25. Meindert Niemeijer, Xiayu Xu, Alina V. Dumitrescu, Priya Gupta, Bram van Ginneken, James C. Folk, and Michael D. Abrámoff, "Automated Measurement of the Arteriolar-to-Venular Width Ratio in Digital Color Fundus Photographs", *IEEE Transactions on Medical Imaging*, Vol. 30, No. 11, November 2011.
26. Daniel Ortíz, Mauricio Cubides, Andrés Suárez, Martha Zequera, Julián Quiroga, Dr. Jorge Gómez and Dr. Nubia Arroyo, "Support System for the Preventive Diagnosis of Hypertensive Retinopathy", 32nd Annual International Conference of the IEEE EMBS, Buenos Aires, Argentina, August 31 - September 4, 2010.

27. Ibaa Jamal, M. Usman Akram, Anam Tariq, “Retinal Image Preprocessing: Background and Noise Segmentation”, TELKOMNIKA, Vol.10, No. 3, July 2012, pp. 537-544.
28. Thomas Walter and Jean-Claude Klein, “Segmentation of Color Fundus Images of the Human Retina: Detection of the Optic Disc and the Vascular Tree Using Morphological Techniques”, ISMDA 2001, LNCS 2199, pp. 282–287.
29. Diego Marín, Arturo Aquino, Manuel Emilio Gegúndez-Arias, and José Manuel Bravo, “A New Supervised Method for Blood Vessel Segmentation in Retinal Images by Using Gray-Level and Moment Invariants-Based Features”, IEEE Transactions on Medical Imaging 2010.
30. Reza Kharghanian and Alireza Ahmadyfard, “Retinal Blood Vessel Segmentation Using Gabor Wavelet and Line Operator”, International Journal of Machine Learning and Computing, Vol. 2, No. 5, October 2012.
31. Safia Shabbir, Anam Tariq, and M. Usman Akram, “A Comparison and Evaluation of Computerized Methods for Blood Vessel Enhancement and Segmentation in Retinal Images”, International Journal of Future Computer and Communication, Vol. 2, No. 6, December 2013.
32. H. Yu, E. S. Barriga, C. Agurto, S. Echegaray, M. S. Pattichis, W. Bauman, and P. Soliz, IEEE Transactions on Information Technology in Biomedicine, Vol. 16, No. 4, JULY 2012.
33. Angel Suero, Diego Marin, Manuel E. Gegundez-Arias, and Jose M. Bravo, “Locating the Optic Disc in Retinal Images Using Morphological Techniques”, IWBBIO 2013.
34. Kiran Yaseen, Anam Tariq, and M. Usman Akram, “A Comparison and Evaluation of Computerized Methods for OD Localization and Detection in Retinal Images”, International Journal of Future Computer and Communication, Vol. 2, No. 6, December 2013.
35. M. Usman Akram, Aftab Khan, Khalid Iqbal, and Wasi Haider Butt, “Retinal Images: Optic Disk Localization and Detection”, ICIAR 2010, Part II, LNCS 6112, pp. 40–49.
36. Anam Usman, Sarmad Abbas Khitran, M. Usman Akram, and Yasser Nadeem, “A Robust Algorithm for Optic Disc Segmentation from Colored Fundus Images”, ICIAR 2014, Part II, LNCS 8815, pp. 303–310.
37. S.G. Vázquez, N. Barreira, M.G. Penedo, M. Rodriguez-Blanco, F. Gómez-Ulla, A. González, and G. Coll de Tuero, “Automatic Arteriovenous Ratio Computation: Emulating the Experts”, DoCEIS 2012, IFIP AICT 372, pp. 563–570.

38. G.Mirsharif, F. Tajeripour, F.Sobhanmanesh, H. Pourreza, T. Banaee, “Developing an au-tomatic method for separation of arteries from veins in retinal Images”, 1st International eConference on Computer and Knowledge Engineering (ICCCKE), October 13-14, 2011.
39. Marc Saez, Sonia González-Vázquez, Manuel González-Penedo, Maria Antònia Barceló, Marta Pena-Seijo, Gabriel Coll de Tuero, Antonio Pose-Reino, “Development of an automated system to classify retinal vessels into arteries and veins”, *Computer Methods and Programs in Biomedicine* 108 (2012) 367-376.
40. D. Relan, T. MacGillivray, L. Ballerini and E. Trucco, “Retinal vessel classification: sorting arteries and veins”, 35th Annual International Conference of the IEEE EMBS Osaka, Japan, 3 - 7 July, 2013.
41. Georgios C. Manikis, Vangelis Sakkalis, Xenophon Zabulis, Polykarpos Karamaounas, Areti Triantafyllou, Stella Douma, Chrysanthos Zamboulis, Kostas Marias, “An Image Analysis Framework for the Early Assessment of Hypertensive Retinopathy Signs”, 3rd International Conference on E-Health and Bioengineering - EHB 2011, Romania.
42. M. U. Akram, S. A. Khan, “Multilayered thresholding-based blood vessel segmentation for screening of diabetic retinopathy”, *Engineering with Computers (EWCO)*, Vol. 29, No. 2, pp. 165-173, 2013.
43. Florian Markowetz, “Classification by SVM”, *Practical DNA Microarray Analysis* 2003.
44. John G. Kohavi R, "Wrappers for feature subset selection", *Artificial Intelligence* 1997, Vol.97, No.1-2, pp.272-324.
45. B. Heinz, J. Gil, D. Kirkpatrick, M. Werman, “Linear Time Euclidean Distance Transform Algorithms,” *IEEE Transactions on Pattern Analysis and Machine Intelligence*, Vol. 17, No. 5, pp. 529-533, 1995.
46. J. Parr and G. Spears, “Mathematic relationships between the width of a retinal artery and the widths of its branches”, *American Journal of Ophthalmology*, Vol. 77, pp.472-477, 1974.
47. Hayreh SS. Optic disc edema in raised intracranial pressure, V: pathogenesis. *Arch Ophthalmol.* 1977;95(9):1553–1565.
48. Quigley HA, Addicks EM, Green WR. Optic nerve damage in human glaucoma, III: quantitative correlation of nerve fiber loss and visual field defect in glaucoma, ischemic neuropathy, papilledema, and toxic neuropathy. *Arch Ophthalmol.* 1982;100(1): 135–146.MedicineNet. WebMD. April 27, 2011. Retrieved August 19, 2011.

49. Binder DK, Horton JC, Lawton MT, McDermott MW. Idiopathic intracranial hypertension. *Neurosurgery*. 2004;54(3):538–552.
50. Frisén L. Swelling of the optic nerve head: a staging scheme. *J Neurol Neurosurg Psychiatry*. 1982;45(1):13–18.
51. Scott CJ, Kardon RH, Lee AG, Frisén L, Wall M. Diagnosis and grading of papilledema in patients with raised intracranial pressure using optical coherence tomography vs clinical expert assessment using a clinical staging scale. *Arch. Ophthalmol*. 2010;128(6):705–711.
52. Lee, Tai S, "Image Representation Using 2D Gabor wavelets" . *IEEE Transactions on Pattern Analysis and Machine Intelligence*, 1996.
53. Xing Wu and Bir Bhanu, "Gabor Wavelet Representation for 3-D Object Recognition" *IEEE transactions on image processing*, vol. 6, 1997.
54. U. Aftab, M. U. Akram, "Automated Identification of Exudates for Detection of Macular Edema", 6th Cairo International Conference on Biomedical Engineering, pp. 27-30, Egypt, 2012.
55. Rafael C. Gonzales, Richard E. Woods, "Digital Image Processing", 3rd Edition.
56. J. Staal, M. D. Abramo, M. Niemeijer, M. A. Viergever and B. van Ginneken, "Ridge-based vessel segmentation in color images of the retina," *IEEE Trans. Med. Imag.*, vol. 23, no. 4, 501-509, 2004.
57. L. Giancardo, F. Meriaudeau, T.P. Karnowski, Y. Li, K.W. Tobin Jr., E. Chaum, "Automatic retina exudates segmentation without a manually labelled training set", *International Symposium on Biomedical Imaging, Russian Federation* (2011).
58. Criminisi A, Perez P, Toyama K. Object removal by exemplar-based inpainting. *CPVR*. 2003;2:721–728.